Biochimica et Biophysica Acta, 976 (1989) 1–27
Elsevier

BBABIO 43038

Review

Excited triplet states used to study biological macromolecules at room temperature

Jane M. Vanderkooi and Jeffrey W. Berger

Department of Biochemistry and Biophysics, School of Medicine, University of Pennsylvania, Philadelphia, PA (U.S.A.)

(Received 2 December 1988)

Key words: Phosphorescence; Excited triplet state; Delayed fluorescence; Anisotropy; Fluorescence

Contents

Abbreviations: DF, delayed fluorescence; Ph, phosphorescence; A, adenosine; IU, iodinated uracil; d, donor; a, acceptor; TT, triplet–triplet; ET, electron-transfer; DMPC, dimyristoylphosphatidylcholine; DOPE, dioleophosphatidylethanolamine; ACh, acetylcholine; EPG, epidermal growth factor.

Correspondence: J.M. Vanderkooi, Department of Biochemistry and Biophysics, School of Medicine, University of Pennsylvania, Philadelphia, PA 19104, U.S.A.

I. Why use excited triplet state molecules?

Fluorescence and phosphorescence are emission processes following the absorption of light. Although both have been observed since antiquity, it was in this century that a distinction between the two was made based upon mechanism. Jablonski suggested that an excited state which is lower lying than the initially excited state could explain multiple emission from a molecule [126]. In the 1940's Lewis and Kasha identified phosphorescence as the light emitted from the triplet excited state [169] and Lewis and Calvin demonstrated the existence of unpaired electrons in the excited triplet state [168]. This definition is now accepted: fluorescence is light emission from a spin-allowed transition whereas phosphorescence is light emission from a spin-disallowed transition. In nearly all cases fluorescence represents the light emitted in the transition from the singlet excited state to the ground state, whereas phosphorescence is light emitted from the triplet excited state to the ground state. Phosphorescence emission is red-shifted and is much longer lived than fluorescence and these features serve to distinguish fluorescence and phosphorescence experimentally.

Fluorescence is now a widely accepted tool for the study of biological molecules. The development of lasers and fast computer-driven data-acquisition devices allows for the measurement of ultra-short fluorescence lifetimes with great accuracy, and fluorescence techniques have addressed fundamental questions concerning molecular motion, distances, orientation and environment.

At room temperature, phosphorescence intensity is lower than fluorescence for almost all molecules, and so the question arises why emission of the triplet state would be of interest. A singlet–singlet transition is spin allowed, and hence occurs rapidly – typically fluorescence decay times are in the nanosecond time regime. In contrast, the triplet–singlet transition is spin forbidden resulting in a long phosphorescence decay, ranging between microseconds and seconds. The long lifetime of the triplet state provides the rationale for its use, allowing phosphorescence to detect and monitor processes that occur on this longer time scale. Slow processes of interest for the function of biological molecules include enzyme turn-over, rotation of lipids and proteins in membranes, motion of large complexes, domain flexibility in proteins and DNA. These processes can be moni-

tored by the *physical* parameters of phosphorescence emission, including spectrum, polarization and lifetime.

Excited states are chemically more reactive than the ground state. Therefore, all molecules in an excited state can be thought of as a new *chemical* species [170]. Whether an excited species will undergo chemical reaction is a function of the excited state lifetime, as well as the mutual reactivity and accessibility of the excited state and neighboring molecules. With this perspective, phosphorescence measurements can also be considered as a chemical relaxation technique in which the reaction is initiated by light, and the reaction kinetics are determined by phosphorescence yield and decay rates.

Phosphorescence from molecules in fluid solutions was observed from eosin in glycerol at room temperature by Boudin in 1930 [24]. Shortly thereafter, Kautsky observed long-lived emission from a variety of organic dyes in deoxygenated solutions [141,142]. In spite of this, it has been a common assumption that phosphorescence can be observed from biological samples only in frozen solution. In recent years this misconception has been abandoned and phosphorescence at room temperature has been receiving attention as a companion tool to fluorescence for the study of biological molecules. We here summarize the recent literature on room temperature phosphorescence to study biomolecules. The chemistry and reactions of the triplet state have been the subject of other reviews [180,194] and an earlier review of phosphorescence to study proteins at room temperature has appeared [121]. Not included in this review is a discussion of the involvement of the triplet state in photoreception including photosynthesis and vision.

II. Overview of factors influencing the appearance and disappearance of the triplet state molecule

IIA. Population of the triplet state

The three-level diagram shown in Fig. 1 depicts the principal processes involved in the population of the triplet state. S_0 represents the ground state and S_1 and T_1 refer to the excited singlet and triplet states, respectively.

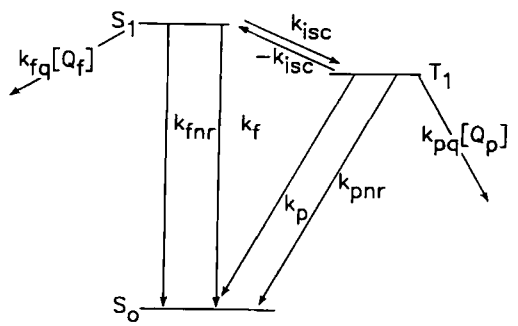

Fig. 1. Energy diagram. S_0 refers to the ground state, S_1 to the excited singlet state and T_1 to the excited triplet state. Transitions occur from the lowest vibrational level (0–0).

The excited triplet state can be populated by several routes. It can be directly excited from the ground state, but a low extinction coefficient associated with the S_0-to-T_1 transition usually makes direct excitation experimentally impractical. Most often, the population of the triplet state is achieved through excitation into the singlet manifold, followed by intersystem crossing to the excited triplet state. Because the singlet state gives rise to the triplet state, fluorescence and phosphorescence have the same excitation spectrum. In an ordinary fluorescence experiment, phosphorescence will also occur, although at room temperature it may be overwhelmed by fluorescence and not be observed.

Energy transfer from a higher state of another species is another means to populate the triplet level. The general scheme for this process is:

$$^3D + A \rightarrow D + {}^3A$$

where D is the donor and A is the acceptor. A review of electronically generated excited triplet species in biological systems is given by Cilento [46].

IIB. Phosphorescence decay

In considering the usual case in which the excited triplet state is populated by absorption of light into the singlet manifold followed by intersystem crossing, the processes involved in forming and removing both the singlet and triplet states will contribute to the phosphorescence yield.

We assume that the absorption of light is instantaneous and that the light intensity is weak so that significant depletion of the ground state does not occur. In addition, it is assumed that the repopulation of the singlet state from the triplet state, described by the rate constant $k_{-\mathrm{isc}}$, is negligible. Referring to the diagram, we can separate the rates that need to be considered for the decay of S_1:

$$\mathrm{d}[S_1]/\mathrm{d}t = -\left(k_f + k_{\mathrm{fnr}} + \sum k_{\mathrm{fq}}[Q_f] + k_{\mathrm{isc}}\right)[S_1] \quad (1)$$

where Q is a quencher species and other parameters are defined in Fig. 1. The summation sign for the collisional quenching term recognizes that more than one type of quencher molecule can contribute to the decay of the single state. The observed singlet lifetime, τ_f, is defined from the decay in fluorescence intensity, I, as:

$$I(t) = I_0 \exp\frac{-t}{\tau_f}$$

and thus

$$1/\tau_f = k_f + \sum k_{\mathrm{fq}}[Q_f] + k_{\mathrm{isc}} + k_{\mathrm{fnr}} \quad (2)$$

The triplet decay is governed by a similar equation:

$$d[T_1]/dt = -\left(k_p + \sum k_{pq}[Q] + k_{pnr}\right)[T_1] + k_{isc}[S_1] \quad (3)$$

Note that in Eqns. 1 and 3 and in Fig. 1 we have distinguished quenchers of fluorescence and phosphorescence, since, in general, the efficiencies of singlet and triplet quenching by a given quencher molecule are different.

In order to significantly populate the triplet state, the rate of intersystem crossing ($T_1 \leftarrow S_1$) must be of the same order of magnitude as the rates of processes converting S_1 to S_0. It follows that the rate of intersystem crossing is fast relative to phosphorescence, so when observing the decay at times longer than microseconds the time required to populate the triplet state can be neglected. The decay is governed by three classes of rates as given by:

$$1/\tau_p = k_{nr} + k_p + \sum k_{pq}[Q_p] \quad (4)$$

When quantum yield of phosphorescence, Φ_p, is considered, the rate of intersystem crossing, k_{isc}, must also be included in the expression:

$$\Phi_p = \frac{k_p \Phi_{isc}}{k_p + k_{pq}[Q_p] + k_{nr}} \quad (5)$$

where the quantum yield of intersystem crossing Φ_{isc} is

$$\Phi_{isc} = \frac{k_{isc}}{k_f + k_{fq}[Q_f] + k_{isc} + k_{fnr}} \quad (6)$$

IIC. Delayed fluorescence

In contrast with 'prompt' fluorescence which arises from the direct population of the excited singlet state, repopulation of the excited singlet state from the triplet state can occur resulting in 'delayed' fluorescence.

One pathway for repopulation of the singlet excited state from the triplet state is by thermal equilibration between the energetically close excited singlet and triplet states. Delayed fluorescence of this type is referred to as T-type (for thermal) or E-type, after eosin, the first molecule observed to emit in this fashion [218]. The yield of T-type fluorescence will depend upon the rate constants of competing reactions:

$$\Phi_{df} = \frac{k_{-isc}\Phi_{isc}\Phi_f}{k_p + k_{pnr} + k_q[Q] + k_{-isc}} \quad (7)$$

The value of k_{-isc} corresponds to the thermal activation to an upper level of the triplet state followed by intersystem crossing to the excited single state. This value is related to ΔE, the energy difference between the emission of fluorescence and phosphorescence, and is related by an Arrhenius equation:

$$k_{-isc} = A \exp(-\Delta E/RT) \quad (8)$$

where A is the frequency factor. ΔE can be determined from the spectra, by measuring the difference in 0–0 energies between fluorescence and phosphorescence.

In cases where thermal equilibration is achieved, the decay rates of delayed fluorescence and phosphorescence are the same and therefore T-delayed fluorescence can be identified as having the same spectrum as prompt fluorescence but the same lifetime as phosphorescence.

The energy difference between the triplet and singlet states for porphyrins is approx. 3100 cm^{-1} [59,79], for proflavin is approx. 2400 cm^{-1} [221] and for eosin is approx. 3100 cm^{-1}. Experimentally, the energy of activation obtained from an Arrhenius plot of the temperature dependence of k_{-isc} agrees with the energy difference obtained from the spectra for chromophores in protein [59] and in DNA [167]. The energy difference between the triplet and singlet states of tryptophan is large: approx. 6800 cm^{-1} and therefore its delayed fluorescence is expected to be very weak at room temperature.

Lee and Galley [167] have pointed out that information can be obtained from the intercept of the Arrhenius plot of the ratio of delayed fluorescence and phosphorescence. Using the expression for delayed fluorescence (DF) and phosphorescence (Ph):

$$\ln\frac{DF}{Ph} = \ln\frac{k_f \Phi_{isc}}{k_p} - \frac{\Delta E}{RT} \quad (9)$$

it is apparent that the intercept is dependent on the quantum yield of intersystem crossing. In a study of proflavin binding to DNA and poly d(A-IU), where A is adenosine and IU is iodinated uracil, these authors observed that the intercept changed, indicating a different intersystem crossing efficiency for the probe in the bound and free state. The value of ΔE measured kinetically was independent of binding, and corresponded to the energy difference of the emission maxima of fluorescence and phosphorescence.

Delayed fluorescence can also arise from triplet–triplet annihilation, and is often called 'P-type' after pyrene [219]. This phenomenon results from the collision of two excited triplet states as follows:

$$T + T \rightarrow S_1 + S_0$$
$$S_1 \rightarrow S_0 + \text{light}$$

In the case of triplet–triplet annihilation, the lifetime of P-delayed fluorescence will be shorter than phosphorescence. In addition, whereas T-delayed fluorescence is independent of the intensity of the excitation light,

triplet–triplet annihilation depends upon the interaction of two excited states, hence its emission intensity will depend upon the light intensity, approaching a dependence upon the square of the power of excitation. Since P-type emission arises from a bimolecular reaction, the yield of P-type emission in fluid solution will also depend upon the viscosity of the solvent. Because close contact between the two species is required, P-delayed fluorescence is less likely to be observed when the chromophore is buried in a macromolecule.

IID. Quenching by neighboring molecules

The quenching of fluorescence by a neighboring molecule has proven to be a powerful tool to measure distances and dynamical processes in macromolecules. Förster energy transfer has often been used as a 'spectroscopic ruler' to measure distances between chromophores [84,260]. Chromophore accessibility, which is related to structural fluctuations in the macromolecule can be revealed by dynamic quenching (e.g., Refs. 65 and 68). Similar protocols using phosphorescence can be devised for obtaining the same sort of information. A review of excited state reactions is given by Turro [265].

Two types of quenching mechanisms need to be considered. First, energy transfer can occur by Coulombic interactions as described by Förster [84]. The energy transfer rate is:

$$k_{\text{Coulombic}} = c\Phi_d\tau_d(K^2/R^6)J_{da} \tag{10}$$

where J is the overlap in spectrum between donor and acceptor, Φ_d and τ_d are the lifetime and quantum yield of the donor, respectively, c is a constant, and K^2 is the orientation factor.

In addition, quenching can also occur via excited state electron exchange. Dexter [56] formulated a theory to describe electron exchange based on wavefunction overlap. The rate of exchange, k_{et}, is given by:

$$k_{et} = K\exp(-2R_{da}/L) \tag{11}$$

where K is related to specific orbital interactions and R_{da} is the donor-acceptor separation relative to their Van der Waals radii, L.

As seen in the Eqns. 10 and 11 quenching by coulombic and electron exchange show different distance dependencies. The exponential dependence on distance shown by electron exchange results in a steeper dependence on distance than for Coloumbic interactions. Therefore, Coulombic interactions tend to dominate at long distance.

The energy exchange mechanism is often considered to be a concerted reaction, in which the electrons are exchanged simultaneously – a triplet–triplet transfer. But alternatively, transfer can proceed through an intermediate diradical following exciplex formation. In some cases there can be a charge transfer, in which a radical ion pair is formed. In ion pair formation there is true electron transfer as opposed to a 'virtual' effect in triplet–triplet transfer.

Both electron transfer and triplet–triplet transfer can be described by the Golden Rule, which expresses the requirement for overlap of the orbitals and the dependence on their coupling:

$$k = 2\pi h^{-1}|V|^2\text{FCWDS} \tag{12}$$

where V is an electronic coupling term and FCWDS is the Franck-Condon weighted density of states [185,187].

A difference between triplet–triplet (TT) and electron transfer (ET) reactions is that for the latter, the rates show strong solvent dependencies due to large changes in the Franck-Condon factors. Triplet transfer, on the other hand, occurs in neutral molecules with little solvent reorganization. Closs et al. [49] compared the rates of TT and ET for a series of molecules in which the donor-acceptor distance was known. From the ratio of rates of the two processes these authors conclude that the simple model viewing triplet transfer as a simultaneous two-electron transfer can be applied.

In Marcus' [186] theory for electron transfer, the rate of transfer, k_{et}, is related to the redox potential, ΔG^0, and the solvent reorganizational energy, λ, according to:

$$k_{et} = A\exp\frac{-(\Delta G^0+\lambda)^2}{4kT} \tag{13}$$

This equation predicts that there will be a ΔG^0 where the rate will be optimal. By using different donor and acceptors with different ΔG^0 the reorganizational energy can be evaluated.

IIE. Influence of diffusion on quenching

When the donor and acceptor molecules are free to diffuse, quenching will be more severe than that predicted by the mean static distances between donor and acceptor.

The simplest description of the quenching of fluorescence for molecules freely diffusing in solution is given by the Stern-Volmer equation:

$$\Phi_0/\Phi = 1+\tau_0 k_q[Q] \tag{14}$$

where Φ and Φ_0 are the fluorescence yields in the presence and absence of quencher and τ_0 is the lifetime in the absence of the quencher [249].

For an exponential decay, lifetimes can be substituted for quantum yields:

$$\tau_0/\tau = 1+\tau_0 k_q[Q] \tag{15}$$

The Stern-Volmer formulation using lifetimes is equally applicable to phosphorescence. However, for the usual case when excitation of the triplet state is achieved by intersystem crossing from the excited singlet state, the analogous equation for intensities (Eqn. 14) can only be used if the quencher does not affect the $S \rightarrow T$ intersystem crossing rate. Phosphorescence lifetimes are often easier to measure than intensities, and therefore Eqn. 15 is usually applied.

When the quenching rate is large, then the quenching reaction will be diffusion limited. The rate will be dependent upon the temperature and viscosity of the solvent according to:

$$k_q = cT/\eta \tag{16}$$

where η is the viscosity of the solvent and c is a constant.

The rate is related to the diffusion coefficient of the reaction species and their encounter distance:

$$k_q = 4\pi r_{ab} N(D_d + D_a) \cdot 10^3 \tag{17}$$

where r_{ab} is the encounter distance, D_d and D_a are the diffusion coefficients of the reactants, and N is Avagadro's number.

We should note that in the above we have ignored the time dependence of the quenching encounter reaction. In a system in which the donor and acceptor are randomly populated, some pairs of molecules will be situated close together and will react rapidly [246]. This will give rise to a fast transient in the decay profile of the donor. Mathematical treatments taking into account the time to establish a diffusion gradient in the case of fluorescence quenching have been presented by several authors [214,282] and experimental application made in membranes and proteins [269,131].

The situation becomes even more interesting when every collision does not produce quenching. For molecules in solution the collision rate of interaction, k_d, the rate of transfer, k_t, and the rate of breakup of the complex, k_{-d}, must be considered:

$$D^* + A \xrightarrow{k_d} D^*A \xrightarrow{k_t} DA^* \xrightarrow{k_{-d}} D + A^*$$

In the case that k_t is very slow relative to k_d the observed rate constant from Stern-Volmer analysis will not be dependent upon diffusion. A slow k_t can arise when the either donor or acceptor is buried in the macromolecule allowing for limited accessibility. As discussed in detail by Thomas et al. [264], the lifetimes will depend upon the quencher concentration and the quencher rate constant as given in Eqn. 14, but the observed k_q will be independent of solvent viscosity.

III. Measurement of phosphorescence

IIIA. Instrumentation

For most samples, the intensity of fluorescence is much higher than that of phosphorescence. Since the fluorescence and phosphorescence emission spectra usually overlap to some extent, most phosphorimeters eliminate the prompt fluorescence through temporal gating. A mechanical shutter is often used for long-lived phosphorescence, as for example described by Strambini [251]. Shorter lifetimes can be measured with flash lamp excitation. When a flash lamp is used, the fluorescence with a lifetime of nanoseconds, will follow the lamp flash, and the long-lived phosphorescence can then be monitored after the lamp flash. With the advent of low-cost computers and analog/digital devices, a phosphorimeter can be readily assembled [101]. In addition, commercially available instruments using xenon flash lamps are available that have time resolution on the scale of milliseconds. Laser-based systems with submicrosecond time resolution are also described in the literature [5,36,88]. An alternative to the pulse method is the phase method, often used in fluorescence measurements [159]. The phase method uses a continuous excitation source, whose intensity is sinusoidally modulated with time. The emitted light is also intensity modulated, but the phase of modulation will be delayed in time and demodulated in intensity with respect to the excitation. From the phase shift and modulation, the lifetime can be calculated. This method has been used to measure lifetimes and anisotropy of triplet probes [87].

The disappearance of the triplet state can be followed optically by monitoring phosphorescence emission. For molecules having more intensity from delayed fluorescence than from phosphorescence, delayed fluorescence provides a more sensitive measurement of triplet state disappearance. Transient absorption also provides a means to follow the disappearance of the triplet state. The transient absorption spectra may reveal intermediates not apparent in the emission spectrum, however. In particular, ionization can give rise to species which may have a similar spectrum and decay time as the triplets. For this reason, it is important to monitor more than one absorption wavelength and, ideally, also the phosphorescence emission.

IIIB. Commonly used phosphorescent probes for ambient temperature

Almost all molecules that fluoresce will also phosphoresce, and there are potentially many suitable phosphorescent probe molecules. However, the ratio of fluorescence to phosphorescence varies greatly from molecule to molecule. In Eqn. 4 we separated the decay of phosphorescence into three contributing rates, namely

the intrinsic rate, the non-radiative rate and the bimolecular quenching rate. Both non-radiative (k_{nr}) and bimolecular quenching (k_q) processes affect the yields of fluorescence and phosphorescence. Incorporation of heavy atoms such as iodide or bromide into an aromatic ring increases the intersystem crossing from the singlet state to the triplet state, resulting in increased phosphorescence [193]. In addition, molecules with carbonyl substituents often show little fluorescence, and high phosphorescence [10]. For molecules which can chelate metals, such as porphyrins, the intersystem crossing rate increases with increasing atomic number of the closed shell metal, affecting lifetime and yields [98]. Because intersystem crossing competes with fluorescence, molecules which are weakly fluorescent can be strongly phosphorescent and vice versa. Non-radiative decay is often enhanced in molecules which have flexible constituents (the so-called 'loose-bolt' effect). Furthermore, distortions of aromatic molecules away from planarity has been proposed to enhance intersystem crossing rates by increasing the mixing of the singlet and triplet states [75]. Therefore distortions can increase the triplet formation, but also increase the rate of phosphorescence decay.

Deuteration of a compound can lead to a dramatic change in phosphorescence lifetime, in contrast with the normally small change in fluorescence lifetime. For instance, at 77 K, the phosphorescence lifetime of naphthalene is 2 s; upon deuteration the lifetime increases to 20 s [245]. The explanation of this phenomenon is that vibrational overtones of the C–H and C–D stretching modes couple with the excited triplet state and promote decay. Many more overtones are needed to match the energy level for the C–D than for the C–H compound and hence coupling is less strong for the deuterated compound and it has a longer lifetime. At room temperature the yield and lifetime of delayed fluorescence and phosphorescence of compounds with exchangable protons can also be enhanced in deuterium oxide solvent. This can be seen for the free-base porphyrins, which have two N–H bonds on the pyroles which can exchange to N–D. The phosphorescence lifetime of porphyrin in iron-free cytochrome *c* at 20 °C is 2 ms in water and 5 ms in ^2H_2O [59].

Consistent with the different electronic structures of ground and excited states, the p*K*'s of excited states differ from the ground state. However, the p*K*'s of the triplet states generally resemble more closely those of the ground state molecule than does the singlet state [217]. For example, the ground state p*K* of acridine is 5.5 and its singlet excited state is 10.6. The p*K* of the triplet state, 5.6, is nearly identical to that of the ground state [127].

IIIB-1. Intrinsic probes

In Fig. 2, the fluorescence and phosphorescence spectra of tryptophan in azurin are shown. At room temperature, some structure in the phosphorescence emission spectrum is evident even though the resolution is decreased by a wide spectral band pass. The phosphorescence intensity is much less than fluorescence, and hence a contribution of phosphorescence cannot be seen in the fluorescence spectrum. An increase in sensitivity of approx. 600 and temporal gating to eliminate the fluorescence was required to obtain the phosphorescence spectrum shown in the figure. The low phosphorescence yield is in part due to a low yield for intersystem crossing. In solution the value of Φ_{isc} is reported to be 0.17 for 3-methylindole and 0.09 for tryptophan [234].

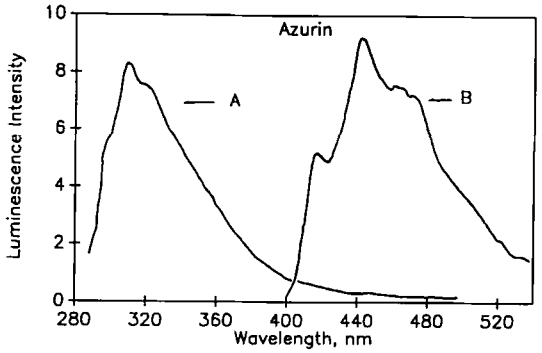

Fig. 2. Fluorescence and phosphorescence of tryptophan. Azurin, 2 mg/ml was dissolved in deoxygenated buffer. Excitation at 265 nm for fluorescence (A) and 270 nm for phosphorescence (B). Phosphorescence (B) was measured with a delay of 4 ms after the excitation flash, using a gate of 2 ms. The relative intensity was approx. 600 times higher for fluorescence. Band pass, 10 nm.

Other structures within cells can phosphoresce. For example, cuprous ion in some proteins shows long-lived luminescence at room temperature. The lifetime of the Cu-CO complex of tyrosine from *Agaricus bispora* was 35 μs with an emission maximum at 530 nm [139] while the Cu-CO complexes of hemocyanin from *Helix pomatia* and *Limulus polyphemus* are longer lived, 70 and 131 μs, and red shifted emitting in the range of 550–560 nm [80].

Vitamin B_6 forms long lived excited triplet states. Lindroth et al. [175] observed that vitamin B_6 cofactor bound to glycogen phosphorylase *b* showed multi-component decay signals.

IIIB-2. Modified intrinsic probes

Heme, the prosthetic moiety of cytochromes, hemoglobin and myoglobin, is composed of an iron surrounded by a porphyrin. The heme is non-luminescent, but the porphyrin can be rendered fluorescent and phosphorescent by removing the iron. The resulting free-base porphyrin can be further altered by incorporating closed shell metals which influence the intersystem crossing rates and hence alter the fluorescence and phosphorescence yields [98].

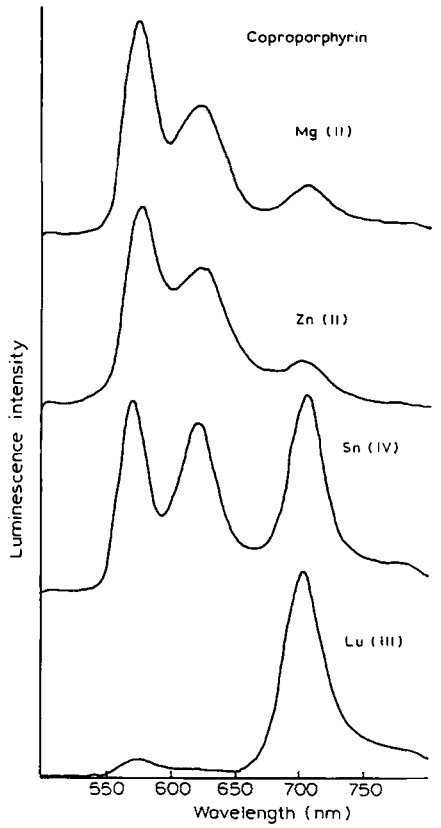

Fig. 3. Delayed fluorescence and phosphorescence of coproporphyrin derivatives. Buffer: Tris-HCl (pH 7). The central metal is indicated on the figure. The phosphorescence and delayed fluorescence were measured using a delay of 0.5 ms after the excitation flash, and a gate of 1 ms. Two peaks at higher energy are delayed fluorescence. Details are in Ref. 273.

Porphyrin-type compounds, including zinc octaethylporphyrin [79], chlorophyll *a* and *b*, bacteriochlorophyll *a* and *c* [220], bacteriochlorophyll [243] and palladium and platinum porphyrins [30], are known to exhibit both phosphorescence and delayed fluorescence at room temperature. Delayed fluorescence from porphyrins is both of the T-type and P-type [30,79].

Enhanced intersystem crossing for porphyrins for the metal series Mg, Zn, Sn and Lu results in decreasing fluorescent lifetimes and increased phosphorescence yields, as seen in Fig. 3. The ratio of phosphorescence/delayed fluorescence also increases in this series, while the phosphorescence lifetime decreases. The room temperature phosphorescence lifetimes are 12, 10, 2 and 0.2 ms, respectively, for the albumin-bound porphyrins in this series. Intersystem crossing yields are high for metal porphyrins. The Φ_{isc} is 0.9 for Zn porphyrin [99] and approx. 1 for Lu porphyrin (our results).

Porphyrins containing metals other than iron are found in tissues in some disease states. The phosphorescence at room temperature from cysticercus of *Taenia solium* isolated from pig and man was used to identify metal-free and Zn porphyrins in this organism [163].

IIIB-3. Extrinsic probes

Fluorescein derivatives are commonly used fluorescent dyes with high fluorescence quantum yields. With bromination or iodination of fluorescein its fluorescence is quenched as the intersystem crossing increases [192]. Eosin (2′,4′,5′,7′-tetrabromofluorescein) has a quantum yield for intersystem crossing in aqueous solution of 0.7 [25]. Erythrosin (2′,4′,5′,7′-tetraiodofluorescein), with a quantum yield for intersystem crossing close to 1, is another commonly used phosphorescent dye [88]. The triplet yields of eosin and erythrosin are dependent upon the environment; the yield is approximately halved when the dye is bound to albumin [88,297]. The spectra of eosin and erythrosin, bound to bovine serum albumin, are shown in Fig. 4. Both exhibit delayed fluorescence and phosphorescence.

DNA conformation has been examined by probes which intercalate into the stack of bases [91,220]. The triplet state of proflavin was used to detect binding to DNA [52,167]. Methylene blue and tetrabromorhodamine 123 bind to DNA by intercalating between base planes in the helix [114,115]. Benzo[a]pyrene adducts of DNA have been detected by room-temperature phos-

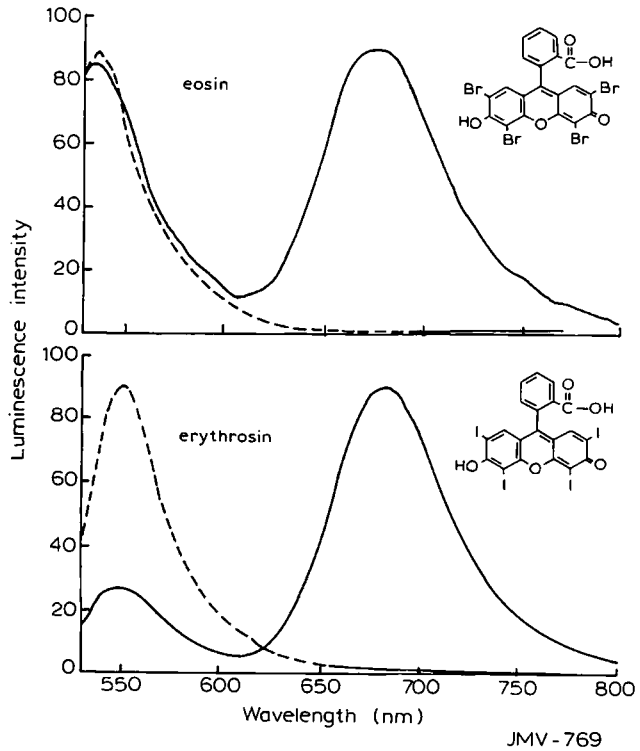

Fig. 4. Prompt fluorescence (------) and delayed luminescence (———) of eosin and erythrosin. The solution contained approx. 1 μM dye and 1 mg/ml of bovine serum albumin in 20 mM phosphate (pH 7). Delayed luminescence was measured with a delay of 0.5 ms after the excitation flash, using a gate of 2 ms. Coincidence of emission maxima of the delayed emission with the prompt fluorescence identifies this emission as delayed fluorescence. Longer-wavelength emission is phosphorescence. The relative intensity for erythrosin fluorescence was about 200 times that for phosphorescence. Details are in Ref. 273.

phorescence [278]. Heterogeneity in DNA-associated solvent mobility was inferred from acridine phosphorescence spectra [198] and the transient absorption of *N*-(1-pyrene)maleimide was used by Lavalette et al. [164] to monitor ribosomal rotational diffusion. Studies of rotational mobility are more fully described in Section VII.

The room-temperature phosphorescence of aromatic hydrocarbons in detergent micelles has been reported [138]. The intensity of phosphorescence is greatly enhanced by the addition of heavy ions Ag^+ and Tl^+ [47,48], or by using probes which have bromide substituents [23]. The commonly used fluorescent probes, anilinonaphthalene sulfonate and toluidylnaphthalene sulfonate bound to bovine serum albumin also exhibit room temperature phosphorescence with low yield [184]. The room-temperature phosphorescence of erythrosin-labeled carbamazepine and other antiepileptic drugs were quenched by antibody specific to the drug [244].

Photoexcited ruthenium complexes with ammonia, bipyridine, or phenanthroline exhibit long-lived luminescence and are strong electron donors. Particular sites on proteins can be specifically labeled [54,213,292]. Long-range electron transfer is indicated on protein [189] or on DNA [227] by surface and intercalated-bound probes.

IV. Intrinsic triplet state molecules: tryptophan phosphorescence used as a probe of protein structure and dynamics

IVA. Most proteins exhibit long-lived phosphorescence

Clues have existed for a long time that proteins phosphoresce at room temperature. In 1746 the great Bologonian scholar, Beccari, concluded that all natural products exhibited luminescence. He saw that the phosphorescence was more pronounced when the sample was cold or dried, and during a cold spell in Bologna, he observed phosphorescence from his own hand [9].

Long-lived excited states in proteins at room temperature were first observed by transient absorption [104]. In 1967 Hastings and Gibson reported that long-lived phosphorescence was observed from bacterial luciferase in the absence of oxygen [109]. In 1974 Saviotti and Galley [242] published spectra from several proteins at room temperature that showed the characteristic vibrational structure of tryptophan phosphorescence. These spectra provided convincing evidence for the observation of phosphorescence from tryptophan-containing proteins at room temperature.

A large number of proteins have now been shown to phosphoresce at room temperature, provided care is taken to remove oxygen. In a survey of 40 proteins, 30 showed phosphorescence lifetimes longer than 1 ms [272]. The literature values for lifetimes of the longest lived component of the protein phosphorescence are given in Table I. Indole compounds in deoxygenated aqueous solutions have a phosphorescence lifetime of approx. 30 μs [13,223]. Thus in the absence of specific quenching, it can be expected that almost all protein tryptophans will be found to exhibit measurable phosphorescence with lifetimes from 30 μs to 5 s.

It is of interest to consider the factors that contribute to the variation in the phosphorescence lifetime of tryptophan in proteins. To understand this, Strambini and Gonnelli [257] have studied the effect of viscosity on the phosphorescence of tryptophan, 1-methyltryptophan, *N*-methyltryptophanamide and tryptophan-containing peptides. The decay rate of the phosphorescence changed by a factor of 100 over a viscosity range of 10^5–1 kPa · s. Out-of-plate distortions will

TABLE I

Phosphorescence lifetimes from tryptophan-containing proteins at approx. 22 °C

Protein	Lifetime (ms)	Ref.
Actin, rabbit muscle	15	120
Albumin, bovine serum	0.9	272
human serum	0.9	272
	0.5	110
chicken egg	15	272
Alcohol dehydrogenase, liver	134	242
	300	31
Aldolase	45	272
Alkaline phosphatase	800	241
E. coli	1500	272
	1700	252
Asparaginase,	50	274
ATPase, sarcoplasmic reticulum	30	272
Azurin	400	272
Cellulase	200	272
Coat protein		
tobacco mosaic virus crystallin	25	14
alpha	5, 42	15
gamma II	9, 93	16
gamma III	11, 75	16
gamma IV	4, 68	16
Edestin, hemp seed	500	272
Glutamate dehydrogenase		
bovine liver	1200	259
E. coli	650	259
Glucose oxidase	120	272
Keratin	1400	165
Lactic dehydrogenase	25	272
Beta-lactoglobulin	15	272
Myosin, rabbit muscle	100	272
Nuclease, micrococcal	400	272
Parvalbumin (with calcium)	5	272
Protease		
Streptomyces griseus	100	272
Bacillus subtilis	10	272
Ribonuclease T_1	14	272
Streptokinase	50	272
Trypsin, bovine pancrease	1.4	137

enhance triplet–singlet mixing, resulting in a decrease in the observed lifetime [180]. Therefore, based upon the viscosity dependence of phosphorescence, it would appear that a long lifetime of tryptophan phosphorescence in a protein may reflect the rigidity of the tryptophan site. Supporting evidence is obtained by comparing fluorescence anisotropy with phosphorescence lifetime. Proteins showing long-lived phosphorescence also show immobilization on the fluorescence time scale including ribonuclease T_1 [205], one of the two tryptophans of liver alcohol dehydrogenase [235] and azurin [225]. In contrast, fast (i.e., subnanosecond) segmental motion is reported for the tryptophan in monellin [162,205], ribonuclease T_1 [71] and mellitin [92], all exhibiting short, i.e., less than 0.5 ms, phosphorescence lifetimes. The membrane protein, myelin basic protein, was not detectably phosphorescent at room temperature when the protein was in solution, but did exhibit phosphorescence when bound to phosphatidylserine vesicles. Although a conformational change could account for the change in phosphorescence yield, it is also possible that the burial of tryptophan in the lipid protects against quenching [267].

Strambini and Gabellieri [253] observed that room-temperature tryptophan phosphorescence from proteins in the solid state, i.e., lyophilized, was intense and long-lived, irrespective of the location of the tryptophan in the protein. The emission intensity and lifetime decreased as the macromolecule was hydrated; water sufficient to form a monolayer on the protein surface produced a decrease in yield and lifetime. The picture from several techniques is that a dehydrated protein has a rigid structure [157,237]. Electrostatic interactions between charged polar groups on the protein surface contribute to the stabilization energy of the tertiary structure whereas motion of the water molecules reduces the electrostatic stabilization energy and contributes to fluctuations in the surface residues [83]. When going from the surface of the protein to the interior, residues tend to become more rigid as indicated by X-ray diffraction analysis [82] and molecular-modeling studies [140]. This again is supporting evidence that rigidity of the site contributes to long lifetime.

For single tryptophan proteins long phosphorescence lifetimes correlate with the relative blue shift of the fluorescence emission [272]. Since blue shift is related to the hydrophobicity of the indole microenvironment, this result also suggests that the longer lived phosphors are more deeply and completely buried.

Because phosphorescence yields and lifetimes are greater in a rigid environment, steady-state phosphorescence measurements at room temperature will tend to select for buried tryptophans in the absence of specific quenching mechanisms. It is noteworthy that the opposite situation exists for fluorescence measurements since, in general, fluorescence lifetimes are longer and quantum yields are higher by a factor of approx. 2–3 for exposed tryptophans than for buried tryptophans [29,103]. Thus steady-state fluorescence measurements tend to emphasize the tryptophans on the surface.

IVB. Relationship between conformation and lifetime

Whereas fluorescence lifetimes of tryptophans in proteins typically vary by about a factor less than 5, the range of phosphorescence lifetimes at room temperature spans 5 orders of magnitude. The great variation in phosphorescence lifetimes allows for the selection of a single tryptophan from a protein containing many tryptophans. It also follows that a change in the conformation of the protein could have a profound effect on the phosphorescence yield and lifetime.

Phosphorescence lifetimes of tryptophans in proteins are highly temperature sensitive [151]. Kai and Imakubo [137] observed that the onset of thermal quenching was protein dependent. Domanus et al. suggested that the ratio of phosphorescence intensity to lifetime be used to characterize this temperature dependence. A step-wise decrease was seen in lifetime/intensity as a function of temperature for the multitryptophan proteins liver alcohol dehydrogenase and alkaline phosphatase but not for free tryptophan or the single tryptophan protein myelin basic protein [60]. These results are interpreted to indicate that the melting temperature of various domains of a given protein are different. Different temperature dependence of phosphorescence yields and lifetimes were observed for phylogenetically distant apomyoglobins, again indicating the sensitivity of phosphorescence to subtle differences in conformation [19].

Protein conformation is altered in the presence of denaturing agents. Gonnelli and Strambini [97,258] followed the phosphorescence of Trp-314 to monitor denaturation by urea of liver alcohol dehydrogenase. As denaturation proceeded, phosphorescence was lost, and the authors attributed the reaction kinetics to a highly cooperative denaturation reaction. Interestingly, the phosphorescence lifetime of Trp-314 is unaffected by crystallization, having nearly the same lifetime, oxygen quenching coefficient and temperature dependence of lifetime as in solution leading Gabellieri and coworkers to conclude [86] that the solution and crystalline conformations must be nearly identical.

The phosphorescence decay of lens alpha-crystallin exhibited two distinct lifetimes corresponding to at least two populations of tryptophan residues in different microenvironments. A discontinuity in Arrhenius plots of the phosphorescence lifetimes between 26 and 29 °C reflected an abrupt transition in segmental flexibility, and measurements in 6 M guanidine-HCl and 8 M urea yielded long-lived components of 3 ms and 7 ms, respectively, suggesting that some structural features of

these exceptionally stable proteins are preserved even in concentrated denaturant solution [15].

The effect of Ca and ATP on the room temperature phosphorescence of the ATPase of the sarcoplasmic reticulum was examined [274]. ATP in millimolar concentrations diminished the phosphorescence intensity by about 30%, an order of magnitude greater than the ATP-induced change in tryptophan fluorescence. The ATP effect on phosphorescence was observed both in the presence and absence of Ca.

IVC. Internal quenchers of the phosphorescence of proteins

Although the rigidity of the site for indole in proteins appears to be a major determinant of the lifetime, quenching moieties within the protein are also likely to influence phosphorescence yield. For example, horse cytochrome *c* with a single buried tryptophan does not exhibit detectable phosphorescence. The tryptophan transfers energy to the adjacent heme by singlet–singlet energy transfer, a process competing with the formation of the triplet state.

Three sulfur-containing amino acids – cystine, cysteine and methionine – exist in proteins. Sulfur-containing compounds can quench phosphorescence. Bent and Hayon [13] showed that RS-SR quenched free indole near the diffusion rate. Calhoun et al. [34] have observed that the sulfur-containing molecules H_2S, CS_2 and ethanethiol quench phosphorescence, as measured by lifetime. The phosphorescence of lysozyme is quenched in the frozen state, but quenching can be eliminated by reducing the sulfhydryls [45]. The effect of sulfur-containing amino acids on room-temperature phosphorescence remains to be determined in model systems and in proteins where Trp–S distances are known.

The possible influence of sulfur-containing moieties on tryptophan phosphorescence was studied by comparing fluorescence and phosphorescence measurements of gamma-II, III, and IV crystallins, three sulfhydryl-rich highly homologous fractions of lens gamma-crystallin. Sulfurs are known to be closest to the tryptophans in gamma-II and most distant in gamma-IV. The fluorescence quantum yield and fluorescence lifetimes increase in the order of II < III < IV, while the phosphorescence yield increases in the order IV < III < II. Sulfur atoms have been shown to promote intersystem-crossing and these results suggest that intramolecular sulfur atoms may be an important determinant of protein phosphorescence yield [16].

Variations in phosphorescence yield due to differences in S–T intersystem crossing rates are suggested from measurements at low temperature. Tryptophan phosphorescence yield at 77 K in rigid solution has a quantum yield of 0.17 [18] but in proteins the yield at 77 K varies from 0.03 to 0.15. (For a comprehensive review, see Longworth [179].) In contrast, the phosphorescence lifetime is relatively constant between 5 and 7 s at 77 K and does not seem to vary significantly between buried and exposed tryptophans [60]. Therefore variation in yield of phosphorescence is due to differences in the $S \rightarrow T$ intersystem crossing rate (Φ_{isc}), as well as the $T \rightarrow S_0$ transition.

V. Quenching by externally added molecules to measure distances and motion in macromolecules

VA. Models of quenching

A basic question, relevant to protein dynamics, is how a molecule in solution can interact with a species buried inside the macromolecular structure. Because of the long lifetime of the triplet state, phosphorescence-quenching studies are especially suited to address this question.

Several different models have been proposed.

(1) The quencher penetrates into the macromolecule. The mathematical treatment of this situation [66–68,100] has been used to analyze oxygen quenching [128].

(2) There is local unfolding. This is the 'gated' model discussed by McCammon and Northrup [191] and applied to fluorescence and phosphorescence quenching by Somogyi et al. [247]. This mechanism and quencher penetration, specifically as applied to H-exchange in proteins, has been discussed by Englander and Kallenbach [76].

(3) The quencher binds [22,69].

(4) The excited triplet state species and the quencher interact by long-range transfer and actual contact between the two is not required. This is suggested by Zemel and Hoffman [299] for porphyrin–porphyrin interactions in proteins. It has also been suggested by Calhoun et al. [34] for protein tryptophan quenching by external quenchers.

The mechanism may depend upon the quencher and the macromolecule under study. Various experimental parameters often need to be varied in order to define the mechanism. For example, penetration (model 1) should be sensitive to size and charge of the quencher [231] but largely insensitive to solvent viscosity [275]. Convincing documentation for long-range transfer (model 4) would require elucidation of the reaction mechanism in terms of predicted distance dependence and redox or spectral behavior (Eqns. 10 and 11).

VB. Oxygen as a quencher of phosphorescence

At room temperature oxygen is the most persistent quencher of phosphorescence and care must be taken to exclude it from the solution. Removal of oxygen can be achieved through a variety of means. Englander et al.

[77] use a combination of dithionite and enzymatic removal employing the coupled enzyme system of glucose oxidase and catalase in the presence of glucose. Strambini recommends deoxygenating by subjecting the sample to a vacuum, followed by reequilibration with nitrogen [252].

The fluorescence and phosphorescence quenching rate constants of oxygen are given in Table II. Considering proteins first, there has been some controversy concerning oxygen quenching constants for tryptophan. This has arisen because of the difficulty in controlling oxygen concentrations in the nanomolar range required for such studies [6,31,34,242,252]. The oxygen present may be photochemically destroyed under illumination of ultraviolet light [31,108,251] or increased by inadvertent contamination from the air. In two laboratories,

TABLE II

Quenching constants for oxygen

Probe	Macromolecule or matrix	Quenching constant ($M^{-1} \cdot s^{-1}$)	Refs.
Fluorescence			
NATA	water	$1 \cdot 10^{10}$	31, 160
Tryptophan	14 proteins	$(2–7) \cdot 10^{9}$	160
	liver alcohol dehydrogenase	$1 \cdot 10^{9}$	73
		$3.5 \cdot 10^{9}$	73
	human serum albumin	$2 \cdot 10^{9}$	160
Pyrene dihydrodiol epoxide	DNA	$9 \cdot 10^{9}$	226
Pyrene	phospholipids	$1 \cdot 10^{9}$	81
Porphyrin	protein	$7 \cdot 10^{8}$	51
Phosphorescence			
Indole derivatives	water	$4 \cdot 10^{9}$	13
NATA	water	$3 \cdot 10^{9}$	72
Tryptophan	parvalbumin (Ca)	$3 \cdot 10^{8}$	34
	melittin (monomer)	$3 \cdot 10^{9}$	93
	melittin (tetramer)	$1 \cdot 10^{9}$	93
	asparaginase	$1 \cdot 10^{9}$	93
	lactoglobulin	$9 \cdot 10^{8}$	34
	ribonuclease T_1	$3 \cdot 10^{8}$	93
	liver alcohol dehydrogenase	$1 \cdot 10^{8}$	93
	glutamate dehydrogenase	$3 \cdot 10^{8}$	252
	bovine	$4 \cdot 10^{7}$	252
	bacterial	$5 \cdot 10^{8}$	252
	aldolase	$4 \cdot 10^{7}$	34
	azurin	$2 \cdot 10^{7}$	34
	human serum albumin	$9 \cdot 10^{7}$	110
	alkaline phosphatase	$2 \cdot 10^{6}$	34
		$1 \cdot 10^{6}$	252
Aromatic hydrocarbons	serum albumin	$\approx 10^{8}$	90
	cyclodextrin	$< 10^{7}$	266
Benzophenone	chymotrypsin	$5 \cdot 10^{6}$	96
Eosin	5 proteins	$3 \cdot 10^{8}$	40
Erythrosin	phosphate buffer	$9 \cdot 10^{8}$	273
	bovine serum albumin	$2 \cdot 10^{8}$	273
Methylene blue	water	$3 \cdot 10^{9}$	17
	DNA, dAdT	$2 \cdot 10^{8}$	17
	DNA, dGdC	$6 \cdot 10^{7}$	17
	nucleosome	10^{9}	116
		10^{8}	116
6 aromatics	DNA	$(1–2) \cdot 10^{8}$	90
Porphyrin	hemoglobin	10^{8}	2
Protoporphyrin IX	water	$1 \cdot 10^{8}$	3
Protoporphyrin IX	myoglobin (glycerol)	$2 \cdot 10^{8}$	3
Zn porphyrin	myoglobin	$2 \cdot 10^{8}$	299
		$1 \cdot 10^{8}$	7
Zn protoporphyrin	water	$1 \cdot 10^{9}$	7
Pd coproporphyrin	water	$4 \cdot 10^{9}$	273
	serum albumin	$1 \cdot 10^{9}$	273

oxygen measurements have now been made by independent techniques, with very close agreement [34,252]. These values are given in Table II.

In examining the data in Table II, it can be seen that when comparing fluorescence and phosphorescence of the same system, the k_q of fluorescence is always higher. For example, the oxygen quenching rate constants of NATA are $1 \cdot 10^{10}$ for fluorescence quenching and $3 \cdot 10^9$ $M^{-1} \cdot s^{-1}$ for phosphorescence quenching [72]. The same pattern is observed for tryptophan in proteins. The respective fluorescence and phosphorescence k_q for liver alcohol dehydrogenase is 10^9 and $3 \cdot 10^8$ $M^{-1} \cdot s^{-1}$ and human serum albumin is $2 \cdot 10^9$ and $9 \cdot 10^7$ M^{-1} s^{-1}. The difference may be due to a statistical factor for phosphorescence quenching by oxygen between 1/9 [95] and 5/9 (reviewed in Ref. 239). Alternatively, if the radius of interaction for fluorescence quenching is larger than the molecular radius, a higher k_q for fluorescence quenching would result.

Ghiron and coworkers [70,93] have compared fluorescence and phosphorescence quenching in seven single-tryptophan proteins. The ratio of phosphorescence/fluorescence k_q's was about 0.2, lower than predicted for diffusion-limited reactions. The energy of activation for phosphorescence quenching was high – about 46 kJ/mol, much higher than the energy of activation of oxygen through an organic solvent. Furthermore, the reaction did not depend upon viscosity of the medium. The authors suggest that the reaction is not difusion-limited and conclude that oxygen quenching is not simply related to protein flexibility.

Although it appears that the oxygen-quenching constants cannot be simply equated with oxygen diffusion, it is nevertheless apparent that rate constants reached for proteins are lower than for NATA by about 20 to 10^3. This result seems in contradiction to the notion that O_2 can diffuse easily through proteins in general. Lakowicz and Weber [161] found that the reduction in quenching in proteins compared to indole derivatives was in the range of 0.17–0.6; however, of the 14 proteins studied by fluorescence-quenching experiments by these workers only azurin is now known to have a single tryptophan, buried and non-exposed.

The binding of aromatic hydrocarbons, including pyrene, benzopyrene, benzanthracene and 7,12-dimethylbenz(a)anthracene, to bovine serum albumin reduced oxygen accessibility [89]. Similar results were found for eosin [40] and porphyrin derivatives [273], showing that polypeptide chains provide some protection from oxygen for these extrinsic probes.

Intercalated dyes in DNA show reduced oxygen quenching, indicating protection of the dyes from oxygen [17,90]. The quenching constants for intercalated methylene blue are less for poly-dGdC than for poly-dAdT, indicating different flexibility or accessibility to oxygen for the two polymers [17].

VC. Quenching by other small molecules

Two other diatomic molecules have been shown to quench phosphorescence of tryptophan. Strambini [252] reported that the k_q for NO quenching of alkaline phosphatase is $8.2 \cdot 10^5$ $M^{-1} \cdot s^{-1}$, which is about the same as the value obtained for oxygen. Therefore, oxygen and NO appear to have about equal access to the tryptophan.

CO quenches phosphorescence of indole, but its efficiency is about three orders of magnitude less than it would be if every collision were effective [34]. The quenching constant was about the same for nine proteins tested.

H_2S quenches the phosphorescence of NATA and of proteins with high efficiency [34]. H_2S is interesting as a phosphorescent quencher in that in size, shape and pK of protonation, it resembles H_2O. The quenching of protein phosphorescence depends dramatically on the pH of the solution. For example, at pH 6, the quenching constant of H_2S for alkaline phosphatase is approx. 10^4 $M^{-1} \cdot s^{-1}$ and at pH 8 the quenching constant is 10^2 $M^{-1} \cdot s^{-1}$. A similar 2–3 order of magnitude decrease in quenching constant was also observed for the buried tryptophans in azurin and LADH. The quenching of NATA by H_2S exhibits little pH dependence, decreasing only about a factor of 3 from pH 5–9. These data would indicate that the charged SH^- cannot easily penetrate to the interior of the protein [290].

VD. Quenching by larger molecules and ions

Larger molecules also quench protein phosphorescence, and for these molecules it is more unlikely that they would penetrate the protein. The phosphorescence quenching of nine proteins by nitrite, ethanethiol, methylvinylketone, nicotinamide, cinnamamide and quinaldic acid was compared by Calhoun and coworkers [34]. The quenching constants varied dramatically from protein to protein, but for a given protein the quenching by the various quenchers were relatively constant. For instance, the quenching constants for the anion nitrite were approx. 10^6 and 10^2 $M^{-1} \cdot s^{-1}$ for parvalbumin and alkaline phosphatase, respectively. Remarkably, the quenching constant for the uncharged species, ethanethiol, was approx. 10^6 for parvalbumin and 10 $M^{-1} \cdot s^{-1}$ for alkaline phosphatase. The similarity in quenching based upon protein and not upon quencher, prompted the authors to conclude that penetration of the quencher into the protein could not account for observed quenching, since penetration by a charged species is predicted to be much less favorable than for an uncharged species. (These quenchers also appear to quench fluorescence by energy transfer, again suggesting that penetration is not required [33].) The quenching also did not show a dependency upon viscos-

ity, which tends to rule out the second model, local unfolding. If phosphorescence quenching can be accounted for by long-range transfer from the protein surface to the buried tryptophan, it can be predicted that quenching efficiency would be primarily determined by the distance of tryptophan from the surface of the protein. Supporting this idea is the observation that quenching is more efficient by larger molecules than by smaller ones. For example, cinnamamide (i.e., vinylacrylamide) is an efficient quencher of phosphorescence [34] whereas acrylamide is inefficient [32,94].

A structural feature of many proteins is their organization into domains, where the domain is a relatively rigid structure which is connected to another domain by a flexible hinge [12]. Rhodanese, a soluble mitochondrial enzyme involved in sulfur metabolism, is one of the simplest of the domain proteins in that it is a monomer and is composed of only two domains. The active site, located in the crevice, has a free sulfhydryl, which allowed for covalent binding with eosin isothiocyanate [154]. The accessibility of various species to the probe was measured by phosphorescence lifetime-quenching studies. The phosphorescent probe was much more accessible to small ions or molecules (iodide and thiosulfate) than to a larger molecule, the spin-label TEMPO. A temperature-induced change in the rate of quenching occurred at around 28° C. It was suggested that fluctuations in the domain displacement resulting in a different accessibility or distance from the surface could account for the results.

The approach that the quenching constant reflects the distance of closest approach between donor and acceptor was used by Yudanova et al. [298] to examine how heme proteins cytochrome *c*, leg-hemoglobin, Met hemoglobin and oxyhemoglobin quenched eosin phosphorescence. They concluded that the quenching efficiency reflected the degree of burial of the heme in the protein. The authors also used delayed fluorescence of perylene and anthracene, probes which partition into the hydrophobic portion of lipid membranes, to see if quenching would be produced by lipid-bound cytochrome *P*-450 and cytochrome b_5. No quenching was observed, and the authors concluded that the porphyrin is protected by the protein matrix.

VI. Modified intrinsic probes: porphyrin metal derivatives used as models for electron-transfer reactions in proteins

A molecule in the excited state will tend to lose an electron because the electron which is moved to an excited orbital is less strongly bound than in the ground state. On the other hand, a vacancy is left in ground state orbital, which can accept an electron. Therefore the excited-state molecule can act both as an oxidant and a reductant. While this is true for both singlet- and triplet-excited states, the longer lifetime of the triplet-state molecule increases the probability of its reaction.

The redox behavior of excited triplet states of porphyrins have been studied extensively, including as a model for photosynthesis and potential use for solar energy [35,118,188,207]. The photochemical properties of excited state porphyrins make them good experimental models to study electron transfer reactions in heme proteins, and we describe here only recent findings as applied to electron-transfer reactions in proteins.

VIA. Hemoglobin hybrids

Mixed-metal [Zn,Fe] hybrid hemoglobins provide a model for porphyrin–porphyrin interactions in which the distance and orientation of all atoms are known by X-ray crystallography. The excited state triplet lifetime of ZnP in Hb hybrids is markedly dependent upon the redox characteristics of the heme in the neighboring chain. At room temperature, the rate constant changes from 55 s^{-1} to 155 s^{-1} when the iron is oxidized [299]. As the temperature is lowered the rate decreases until approx. 160 K, when the rate becomes temperature independent. The details of the reaction depend upon whether the alpha or beta chain is substituted due to temperature-dependent change in ligation of the iron [224]. The reorganization energy λ was about 2.3 eV.

VIB. Zn myoglobin and anthraquinone

The quenching rate of delayed fluorescence of Zn-protoporphyrin myoglobin by anthraquinone sulfonate was determined by Barboy and Feitelson [7] to be $2 \cdot 10^8$ $M^{-1} \cdot s^{-1}$ with $E_{act} = 24$ kJ mol. The k_q was only about one order of magnitude less than for oxygen and the authors suggest that anthraquinone sulfonate can diffuse through the protein. However model studies have indicated that excited state porphyrins can interact with quinones over distances up to 1 nm [174]. Based on the model studies, the findings of Barboy and Feitelson could also be interpreted with the view that long-range transfer occurred, without penetration of the anthraquinone.

VIC. Cytochrome c and b_5

Zn cytochrome *c*, the derivative of cytochrome (Cyt) *c* in which iron is replaced by Zn, is a strong photoreductant, reacting with ferricyanide and methylviologen [122,279]. The redox potential of the couple ^{3}Zn(Cyt *c*)/Zn(Cyt *c*)$^+$ is given by McLendon and Miller [196] to be 0.75 V. The excited triplet state of Zn cytochrome *c* is quenched by cytochrome b_5 with a rate constant of $5 \cdot 10^5$ $M^{-1} \cdot s^{-1}$ in an electron-transfer mechanism [197]. McLendon and Miller [196] compared the rates of electron transfer between metal-free and metal deriva-

tives of cytochrome *c* and cytochrome b_5 with the predicted redox behavior of Marcus' [186] theory. The reorganization energy, λ, was determined to be 0.8 eV. This is a rather large value, and the authors suggest that the polypeptide chain plays a role in the electron-transfer process.

VID. Cytochrome c and cytochrome c peroxidase (CCP)

The complex between CCP and cytochrome *c* is one of a few biological redox pairs in which the three-dimensional structure of each of the partners has been determined. Several groups have prepared derivatives in which iron was replaced by zinc or other closed-shell metals [111,155,171–173,270,293].

Electron transfer between Zn CCP and yeast cytochrome *c* was demonstrated by the transient absorbance spectra [173]. The rate differs with the type of cytochrome *c* used being about 100 times faster for yeast cytochrome *c* than for the horse derivative [111], and varies with amino-acid-substituted mutants of cytochrome *c* [172]. For aromatic substituents at amino acid position 82 the rate of the reaction $^3ZnP \rightarrow Fe(111)P$ was between 150 and 175 s^{-1}. With aliphatic substituents at the same position, the rates were less, ranging from 13 to 95 s^{-1}. The rate of the dark back reaction ($Fe(II)P + ZnP^+ \rightarrow ZnP + Fe(III)P$), in contrast, was about 10^4 faster for the aromatic than for the aliphatic substituents. These experiments help to emphasize the important role that the polypeptide chain has in determining the kinetic parameters of the reaction.

Koloczek et al. [155] compared the interaction between Sn and Zn cytochrome *c* with CCP. The phosphorescence of Zn but not Sn cytochrome *c* shifts by about 20 nm to the blue upon complexation to CCP or apo-CCP. One explanation for the shift to higher energy would be due to an increased binding or torsion of the Zn cytochrome *c* porphyrin ring in the protein. Interestingly, Sn cytochrome *c* has no such detectable shift in emission maximum. The Sn porphyrin molecule in the crystal state is C_{4h} with tetragonal symmetry. Zn porphyrin in the protein is a square-pyramidal five-coordinated structure (C_{4v}). The Zn porphyrin may be more susceptible to distortions which would alter the emission properties.

VIE. Zn cytochrome c–cytochrome c interactions

At high ratios of Zn cytochrome *c* to poly-l-aspartic acid it was observed that quenching of phosphorescence occurs, but not at low ratios [155]. This behavior was attributed to interaction of bound excited state molecules with closely bound neighboring ground state molecules, since it is known that porphyrins free in solution can self-quench at low concentrations [79,273]. When the porphyrin is surrounded by protein the rate of interaction is much less and high concentrations are needed for significant quenching to occur, but such an effective concentration was obtained when the positively charged cytochrome bound to the negatively charged polyaspartic acid.

VIF. Triplet state porphyrins and cytochrome c

Cho et al. [44] have compared the electron transfer between ferric cytochrome *c* and excited triplet states of various Zn and free-base porphyrins. Both the oxidation and reduction rates could be determined. The reorganizational energy was 1.0 eV, somewhat smaller than 2.3 eV found by Peterson-Kennedy et al. [224] for metal derivatives of hemoglobin.

VIG. Horseradish peroxidase and aromatic substrates

Horseradish contains eight different isozymes of peroxidase, with subtle enzymatic differences. The phosphorescence emission of iron-free isoenzyme HRP-A and HRP-C were compared [123]. The triplet lifetime at 20 °C was 4.8 and 5.5 ms for HRP A and C, respectively. Addition of substrate, naphthalene hydroxamic acid, decreased both lifetimes, indicating proximity to the porphyrin ring.

VII. Triplet-state measurements of rotational motion

VIIA. Principle

Fluorescence techniques have been widely used to study nanosecond and subnanosecond molecular motions (see, for example, Refs. 162, 205 and 291). In contrast, triplet state techniques provide a convenient window for dynamical studies on the microsecond and millisecond time scales. Reviews of the use of long-lived transients to measure rotation are available [132].

Like fluorescence, phosphorescence is polarized. In the anisotropy decay experiment, linearly polarized excitation photoselects an anisotropic distribution of lumiphores which are then free to diffuse rotationally and translationally. The anisotropy is a function of the parallel, I_p, and perpendicular, I_s, components of the luminescence emission,

$$r(t) = \frac{I_p(t) - I_s(t)}{I_p(t) + 2I_s(t)} \tag{18}$$

and details regarding rotational diffusion can be extracted from the anisotropy decay according to theory described elsewhere [250,280].

Theoretical descriptions of phosphorescence depolarization are derived from the extensive literature describing fluorescence anisotropy and Brownian rota-

tional diffusion [11,74,78,222,262,283–285]. Since phosphorescence techniques are most suitable for dynamical regimes with long correlation times, much emphasis is placed on the theory describing hindered motions, as in membrane bound systems [1,85,148,149,176,177,261].

Kinosita et al. [148] characterized the dynamics of a membrane-bound fluorophore by (1) the wobbling diffusion constant, D_w, and (2) the degree of orientational constraint. In principle, both parameters can be derived from the anisotropy decay experiment; D_w is a function of the initial slope of $r(t)$, and the limiting anisotropy is dependent on the conical angle of constraint.

Cherry [36,37], following the analysis of Rigler and Ehrenberg [233], described a simpler model where the membrane-bound moiety is permitted to diffuse rotationally about an axis parallel to the membrane normal, but rotational diffusion is negligible about axes in the plane of the membrane. In this formulation

$$r(t) = A_1 \exp(-D_p t) + A_2 \exp(-4D_p t) + A_3 \tag{19}$$

where D_p is the diffusion constant for rotation about an axis parallel to the membrane normal. In the transient absorption experiment, the coefficients A_i are simply a function of the angle θ between the absorption transition moment and the membrane normal

$$A_1 = 1.2(\sin^2\theta \cos^2\theta)$$

$$A_2 = 0.3 \sin^4\theta \tag{20}$$

$$A_3 = 0.1(3\cos^2\theta - 1)^2$$

The diffusion coefficient, D_p is a function of particle size and membrane viscosity. Saffman and Delbruk [238] modeled the membrane-bound moiety as a cylinder with its axis of symmetry parallel to the membrane normal, and derived an explicit formula for the diffusion coefficient

$$D_p = \frac{kT}{4\pi a^2 h \eta} \tag{21}$$

where a is the radius of the cylinder, h is the length immersed in the membrane, and k, T and η are Boltzmann's constant, the absolute temperature, and the membrane viscosity, respectively.

The initial polarization is a function of the angle between the absorption and emission dipole moments. For tryptophan, the phosphorescence emission dipole is nearly perpendicular to the absorption dipole resulting in a negative polarization of $r = -0.2$ [156], while the limiting anisotropy of eosin or erythrosin immobilized in polymethylmethacrylate is about 0.25 [88].

VIIB. Technical aspects of measurement of rotation by triplet-state spectroscopy

Rotation of a triplet state probe can be directly measured by phosphorescence anisotropy [5,88,133,200]. In cases where delayed fluorescence is stronger than phosphorescence, the anisotropy of delayed fluorescence can be used [102]. Transient polarized absorption of the triplet state molecule is also commonly used [5,36,37]. In this method a pulse of light transiently populates the lowest triplet state, while the dichroism of a probe beam tuned to the triplet–triplet transition is measured. The high resolution of absorption measurements affords this method great sensitivity; however, this technique is somewhat more complex than direct phosphorescence anisotropy decay measurements in that two beams are required. A third technique, polarized fluorescence depletion, has also been implemented. Originally applied to microscopy [129,130], this technique measures the depletion and recovery of polarized fluorescence intensity after an asymmetric depletion of the ground state with linearly polarized excitation [53,285,294]. For probes with high rates of intersystem crossing, the fluorescence depletion is significant, and, because fluorescence has a higher quantum yield than phosphorescence, this method combines the sensitivity of fluorescence measurements with the long lifetime of triplet states, with sensitivity sufficient for single cell measurements. This method has recently been applied in frequency domain, where the frequency shifts between modulation in excitating light and the emission is detected [295];excellent agreement between theory and experiment has been obtained for model systems.

The first rotational diffusion measurements of a membrane-bound protein were reported by Cone [50]. This measurement did not involve a triplet state, but the experimental techniques are the same as for triplet state measurements. By exploiting the intrinsic chromophore, 11-*cis*-retinal, of the visual protein rhodopsin, rotational relaxation times were measured in rod outer segment membranes. Upon excitation, rhodopsin photochemically converts to a long-lived intermediate – lumirhodopsin – and transient dichroism measurements of this species yielded a rotational relaxation time of 20 μs at 20 °C. A similar approach was used to study rotation of bacteriorhodopsin [41–43]. Razi Naqvi et al. [228] observed no dichroism change during the lifetime of the transient, suggesting that the chromophore is highly immobilized within the membrane.

We now review studies of segmental flexibility and rotational motion of biological macromolecules as probed by intrinsic and extrinsic triplet state probes. Intrinsic probes offer the advantage that structure and conformation are not disrupted; however, intrinsic probes often have low triplet yields. Extrinsic probes with high triplet yields can often be introduced; how-

ever, the degree to which binding may alter the native conformation is usually unknown.

VIIC. Systems studied by intrinsic probes

VIIC-1. Tryptophan

Strambini and Galley [255,256] reported the detection of slow rotational motions of proteins in viscous solution as measured by the anisotropy decay of the native tryptophan phosphorescence at −90 to −70 °C. Kim and Galley [147] described similar low-temperature measurements of human serum lipoproteins, and the rotational correlation times were consistent with molecular-weight-based estimates of protein size. Strambini et al. [259] derived the rotational correlation times for bovine liver and *Escherichia coli* glutamate dehydrogenase using steady-state phosphorescence anisotropy measurements and the calculated molecular masses of 345 and 293 kDa were in good agreement with known molecular masses of 336 and 270 kDa for the bovine and bacterial enzymes, respectively.

Strambini and Gabellieri [254] measured the steady-state phosphorescence anisotropy of crystalline LADH Trp-314 at 20 °C, and observed no loss in anisotropy during the emission lifetime of 500 ms. The authors concluded that the indole side chain is immobilized on the time scale of 1 s. Berger and Vanderkooi [14] observed the time-resolved phosphorescence anisotropy of the tobacco mosaic virus by measuring the tryptophan phosphorescence of the coat protein. In 85% glycerol at 5–20 °C, the biphasic anisotropy decay was found to be consistent with the size and shape of the cylindrical virus.

VIIC-2. Heme proteins

An elegant optical method to measure rotation of heme proteins is to use the anisotropy of the polarized absorption following photolysis with polarized light of the CO-adduct of heme. This method is limited to those heme proteins that bind CO, including cytochrome oxidase [135,136,143–146,158] and cytochrome *P*-450 [106,107,195,232]. For heme proteins which do not form CO complexes, the strategy has been to substitute iron with a metal which renders the porphyrin phosphorescent by promoting intersystem crossing, and then to use triplet state anisotropy techniques to measure rotation.

Vaz et al. [277] substituted rhodium (III)-protoporphyrin IX for the native heme group in the integral membrane protein cytochrome b_5. After incorporation into liposomes, biphasic anisotropy decay curves were measured both above and below the lipid phase transition. Rotational correlation times as derived from the fast components were $1.1 \cdot 10^4$ s^{-1} at 10 °C, and $2.4 \cdot 10^5$ s^{-1} at 35 °C, and the molecule was found to wobble in a cone having a semiangle of 34°.

The molecular motion of metal-substituted cytochrome *c* derivatives was examined using fluorescence and phosphorescence anisotropy by Dixit et al. [57,58]. For mitochondrial-bound cytochrome *c* there was no decay in the fluorescence anisotropy, indicating that cytochrome *c* does not rotate in the nanosecond time scale. The phosphorescence anisotropy decayed with a correlation time constant of 300 μs and a second long-lived component, which could be accounted for by the rotation of the entire mitochondrian. The anisotropy decay could be fit to a model where the protein performs a restricted rotation in a cone about a single axis. An alternative explanation is that there is a population of cytochrome *c* molecules which are free to rotate, whereas others are immobilized. An immobilized fraction is suggested by measurement of lateral diffusion using fluorescence recovery after photobleaching (Refs. 112 and 271, but see also Ref. 105).

VIID. Systems studied by extrinsic probes

The fluorescein derivatives eosin and erythrosin have high triplet yields and phosphorescence lifetimes on the order of 0.1–1 ms, hence these probes can be used effectively to measure rotational relaxation times on the order of 10^{-5}–10^{-3} s [88]. Cherry et al. [40] described the preparation of the triplet probe eosin isothiocyanate, and Cherry and Schneider [38] confirm the validity of using bound eosin to probe rotational motions on the microsecond and millisecond time scales. Moore and Garland [199] discuss the preparation of erythrosin isothiocyanate and review its suitability as a probe for dynamical processes. The photophysical properties of fluorescein, eosin, and erythrosin have been summarized [133] and several applications are considered below.

VIID-1. Band-3 protein of the human erythrocyte

Band-3 proteins of erythrocyte ghosts were the first membrane-bound proteins to be studied with polarization measurements of triplet probes [39,212]. Band 3 has a molecular mass of approx. 90 kDa, comprises roughly 25% of the total membrane protein, and functions as an anion transporter. Cherry and his co-workers [39,211] studied the rotation of band-3 proteins by flash photolysis and transient absorption measurements of eosin isothiocyanate-labeled proteins. Initial results confirmed that band-3 proteins diffuse rotationally about an axis normal to the membrane plane with a diffusion constant of 10^3 s^{-1}. Further experiments deduced the coexistence of both slowly and rapidly rotating forms of band-3 proteins. The equilibrium between the two forms is temperature dependent with the slowly rotating form favored at low temperatures, suggesting that temperature-dependent protein–protein associations can significantly influence membrane dynamics [208,209]. Proteol-

ysis studies subsequently confirmed this finding, and it was found that up to 40% of band-3 protein is linked to the erythrocyte cytoskeleton [210]. Aggregation was also influenced by proteins and peptides which bind to band 3 [62,63] and by cholesterol [201]. The temperature- and concentration-dependent self-associations were observed in reconstituted lipid vesicles [202,205] to be consistent with observations in intact erythrocyte membranes.

VIID-2. Glycophorin

Glycophorin, the major sialoglycoprotein of the human erythrocyte membrane, has been studied in order to understand lipid–protein interactions and their role in biomembrane structure and function. Glycophorin has a molecular mass of 30 kDa; however, the aggregation state is dependent on the lipid used in reconstitution [276]. Phosphorescence depolarization measurements of glycophorin labeled with erythrosin isothiocyanate have been used to study the rotational mobility of this integral membrane protein. Jovin et al. [133] measured the phosphorescence anisotropy decay of labeled glycophorin in 99% glycerol, and in reconstituted dimyristoylphosphatidylcholine (DMPC) vesicles. In 99% glycerol, glycophorin exhibited rotational correlation times over the 1 μs to 1 ms time-scale and a non-zero residual anisotropy. These results reflect both very fast segmental flexibility, and the existence of large aggregates. In DMPC, correlation times in the 1–2 μs and 10–20 μs range were observed along with a high limiting anisotropy, corresponding to significant segmental flexibility and the formation of very large aggregates. The initial and residual anisotropies decreased with increasing temperature, reflecting a temperature-dependent aggregation state.

Van Hoogevest et al. [276] examined the rotational mobility of glycophorin in various lipid vesicles. With the exception of DMPC at the phase transition (22° C), no decay in the anisotropy was observed in the 1–300 μs range. In liquid crystalline dioleophosphatidylethanolamine (DOPE), bovine brain phosphatidylserine and DMPC, a static anisotropy of 0.01 was measured. For gel state DMPC, DOPE, and DMPC upon the addition of the aggregating agent wheat germ agglutinin, a constant anisotropy of 0.03 was measured. The authors suggest that an anisotropy level of 0.03 corresponds to slowly rotating aggregates ($t_c > 0.3$ ms), while an anisotropy level of 0.01 corresponds to segmentally flexible glycophorin ($t_c < 1$ μs). These results indicated the influence of lipid composition on the aggregation state of the protein.

VIID-3. Lactose permease

Lactose permease is an integral membrane transport protein. Radiation inactivation studies have suggested that the permease exists as a monomer in the absence of membrane potential, but as a dimer in the presence of a membrane potential. The phosphorescence anisotropy decay was measured in order to determine the rotational diffusion coefficient and molecular size [61]. *E. coli* lactose permease was labeled with eosinylmaleimide and reconstituted into lipid vesicles. In contrast with radiation inactivation studies, phosphorescence anisotropy measurements suggest that the enzyme exists in the membrane as a monomer both in the presence and absence of membrane potential.

VIID-4. Acetylcholine receptor

Acetylcholine receptors densely cover the post-synaptic terminal of the cholinergic synapse, and its molecular organization has been a topic of intense interest. Lo et al. [178] studied the mobility of ACh receptors in the torpedo electric organ by measuring the phosphorescence polarization of alpha-bungarotoxin covalently labeled with erythrosin-isothiocyanate and subsequently bound to the receptors. It was found that, in situ, the receptors are immobilized on the millisecond time scale, but that alkali extraction permits significant rotation. Bartholdi et al. [8] examined the microsecond time scale using eosin derivative probes, and found rotational correlation times of 10–26 μs compatible with the 9-S monomeric receptor species at 22° C, and alkaline-treated membranes at 39° C. In contrast, *N*-ethylmaleimide-treated membranes not subjected to alkaline treatment were more rigid, and did not exhibit microsecond anisotropy decay components.

VIID-5. Mitochondrial ADP/ATP translocator

The ADP/ATP translocator is a specific carrier that catalyzes the translocation of one ADP for one ATP across the inner mitochondrial membrane. It is defined by the binding of substrates, ADP and ATP, or the highly specific inhibitors, atractylate, carboxytractylate and bongkrekate [152]. Müller et al. [203] have examined the rotational diffusion properties of the ADP/ATP translocator in the inner mitochondrial membrane by labeling the translocator selectively with eosin-5-maleimide and monitoring the flash-induced transient absorption anisotropy. They observed a rotational time of 100 μs at 37° C and 240 μs at 5° C. There was a time-independent phase in the anisotropy decay with the measured time scale of approx. 500 μs. The latter was attributed to an immobile fraction of the translocator. Since the translocator maintains a fixed orientation with respect to the plane of the membrane [26], the mobile fraction is interpreted to indicate that the protein rotates on a single axis normal to the membrane plane. Müller et al. [204] also showed by fluorescence anisotropy that the eosin probe undergoes rapid wobbling motion on the subnanosecond time-scale.

VIID-6. Ca-dependent adenosine-5′-triphosphatase of sarcoplasmic reticulum

The Ca-ATPase of the sarcoplasmic reticulum serves to regulate the level of Ca in muscle during the contraction-relaxation cycle. Because of the dual function of the ATPase in release of calcium during contraction and the sequestering of Ca during relaxation, the activity of the ATPase is highly regulated. One suggestion, that aggregation of monomers play a role in the regulation of this enzyme, could be tested by phosphorescence anisotropy techniques.

Hoffmann et al. [113] labeled the protein with eosin isothiocyanate and measured rotational motion by the flash-induced dichroism of the transient triplet state. The Arrhenius plot for rotational mobility displayed discontinuities at 15 and 35 °C while the Arrhenius plot for enzymatic activity exhibits a transition at 15 °C. It is proposed that a sudden conformational change in the ATPase at 15 °C accounts for the abrupt change in activity, and this notion is supported by the strong correlation between the activation energies for rotational mobility (141 ± 9 kJ/mol) and enzymatic activity (142 ± 17 kJ/mol) above the transition.

Burkli and Cherry [27] observed rotational motions of the ATPase after 20 μs and reported a small value for r_0 indicative of protein segmental flexibility. The anisotropy decays with a temperature-dependent time constant of 90 μs at 0 °C, and 40 μs at 37 °C, and this component is assigned to rotation about an axis normal to the membrane plane. Rotational anisotropy increased upon fixation with glutaraldehyde, and this result was confirmed with the steady-state measurements of Murray et al. [206]. The results of Speirs et al. [248] are in general agreement with Burkli and Cherry [27] and, in addition, a fast depolarization on the order of 1–5 μs was observed and attributed to protein segmental motion. Temperature-dependent studies suggest that the onset of structural changes in the ATPase occur at 11–13 °C.

Restall et al. [229] observed a submicrosecond decay component, and proposed a model where the phosphor itself reorients on a submicrosecond time-scale about an axis attached to a larger domain, which in turn rotates on a time-scale of a few microseconds. A fraction of the proteins are then free to rotationally diffuse in 100–200 μs, while a fraction remains fixed on the submillisecond time-scale. A change in the anisotropy upon calcium addition was interpreted in terms of a conformational change [230].

VIID-7. Viral glycoproteins

The molecular events responsible for the viral fusion process are not well characterized. Since gross conformational changes must accompany fusion, it is likely that viral mobility facilitates the fusion event. In order to test this hypothesis, the rotational mobility of sendai virus [166] and influenza virus [134] glycoproteins have been investigated.

Sendai virus is a paramyxovirus characterized by two glycoproteins surrounded by a lipid envelope. Lee et al. [166] investigated the rotational mobility of sendai virus glycoprotein by flash induced transient dichroism of eosin probes. An anisotropy component of 100–200 μs was observed at 37 °C, and this component was assigned to overall rotation about an axis normal to the membrane surface. Low values of initial anisotropy were interpreted to reflect glycoprotein segmental flexibility. The temperature dependence of the segmental and rotational motions exhibited a sharp increase at 30–35 °C paralleling the temperature dependence of virus-induced hemolysis, suggesting that fusion activity and rotational mobility are correlated.

Junankar and Cherry [134] studied the mobility of spike glycoproteins in influenza virus (strain X-47) as a function of temperature and pH in order to correlate mobility with hemolytic activity. The mobility of the glycoproteins exhibited a strong temperature dependence which paralleled the hemolytic activity similar to that observed for sendai glycoproteins. pH measurements showed greater mobility at pH 7.3 than at pH 5.2 (where hemolytic activity is maximal); however, it is proposed that low pH inactivation of the influenza virus restricts the mobility before a mobility measurement can be made. The authors speculate that mobility is increased at pH 5.2 immediately after lowering the pH.

VIID-8. Epidermal growth factor (EGF)

EGF is one of a family of low-molecular-weight polypeptide growth factors. Zidovetzki and coworkers [300–302] and Jovin [132] prepared the erythrosin-EGF conjugate which is biologically active and shows high phosphorescence. At 4 °C, the rotational correlation times ranged from 25 to 90 μs for EGF bound to the receptor of human epidermoid carcinoma cells, or to isolated plasma membranes. At higher temperatures and longer incubation times the rotational time increased up to 75 μs for the isolated membranes and 350 μs for the cells. The authors attribute the increase to an aggregation of the occupied EGF receptors.

VIID-9. Myosin

It is proposed that rotational motions of myosin are intimately connected with force generation during muscle contraction. Dynamical measurements of cross-bridges have exhibited a wide range of correlation times from 10^{-9} to 1 s [28]. Triplet state techniques have identified motions principally in the microsecond range [182].

Eads et al. [64] examined the rotational motion of myosin on the microsecond time scale by time-resolved anisotropy of absorption and phosphorescence of an eosin probe bound to the reactive $-SH_1$. Isolated S_1

fragments at 4°C exhibited a rotational correlation time of 210 ns consistent with S-1 tumbling. Actin binding was observed to restrict mobility greatly. Anisotropy measurements of myosin monomers yield correlation times of 400 ns, and 2.6 μs. The long-lived component contradicts the 'free-swivel' model for S_1 and suggests a restricted motion. Synthetic thick filaments exhibited correlation times of 700 ns and 5 μs demonstrating that motions are slower and more restricted in the filaments than in the monomers. It is suggested that the submicrosecond motions reflect flexibility at the S-1–S-2 junction and that the flexibility at the junction between S-2 and the light meromyosin results in correlation times of several microseconds.

Kinosita et al. also observed both slow and fast components of the anisotropy decay in myosin synthetic filaments [150]. In addition, temperature-dependence studies showed no gross conformational changes between −10 and 20°C. The submicrosecond decay was modeled as a wobbling-in-a-cone motion of the head within a cone of semiangle of 35° for the filament and 41° for the solubilized proteins. The slow component was assumed to result from a wobbling contribution of the rod. Analysis suggested that 14 nm of the rod rotates in a cone of 48° for the filament and 57–60° for the solubilized proteins.

Ishiwata et al. [125] observed myosin rotation in rabbit microfibrils and again reported both fast (submicrosecond) and slow (several microseconds) anisotropy decay components. By applying the double cone model, conical semiangles of 30° and 50° were derived for the fast and slow rotational modes, respectively.

Ludescher and Thomas [181] reported complex rotational motions of the myosin heads in rabbit myofibrils. Correlation times of 5 and 40 μs were observed and the motion was bounded, as demonstrated by a non-zero value for the residual anisotropy out to 1 ms. By extending the time-scale, the long-lived correlation component could be detected which was not observable in previous studies. In agreement with past work, longer correlation times and higher residual anisotropies were measured for myofibrils in comparison with heads in filaments, confirming the dynamical constraints within the myofibril. In addition, a constant anisotropy is reported for heads in rigor. Recent studies on the rotational dynamics of myosin filament cross bridges have demonstrated that the rotational dynamics of myosin heads in thick filaments are sensitive to pH, ionic strength and Mg^{2+} in the physiologically relevant regime [183]. At pH 8.2, 0.1 mM Mg^{2+}, the anisotropy decayed to a limiting value of 0.038 with correlation times of 0.5 and 3.8 μs. In 10 mM Mg^{2+}, the correlation times of 0.6 and 5.7 μs and limiting anisotropy of 0.055 were measured.

VIID-10. Actin

Sawyer et al. labeled Cys-374 of rabbit muscle actin with erythrosin iodoacetamide [241]. Phosphorescence anisotropy decay measurements of F-actin at equilibrium yielded anisotropies ranging between 0.035 and 0.08 dependent on the actin concentration with no anisotropies ranging and spectrin-binding proteins resulted in increased r_0 reflecting a more completely immobilized chromophore; furthermore, changes in rotational correlation times could be detected during polymerization. Details of the polymerization reaction did not agree with previous results of Yoshimura et al. [296] which may reflect the preparation of the samples.

VIID-11. Lipids and lipoproteins

Blatt and Corin examined the phosphorescence properties of two eosin-labelled fatty acids of different alkyl chain length in dimyristoylphosphatidylcholine vesicles [20]. Eosin was labeled at the head of fatty acids with 12 (E12) and 16 (E16) carbons. The divalent cation Cu^{2+} quenched E12 preferentially, while the hydrophobic molecule, *N,N*-dimethylaniline, preferentially quenched E16, and therefore it appears that E16 is buried deeper into the hydrophobic core of the membrane. Above the phase transition the phosphorescence anisotropy decayed monoexponentially with a rotational relaxation time of around 50 μs, but the anisotropy did not decay to zero. Below the phase transition the decay was multi-exponential. The authors suggest that the eosin probe has hindered rotational motion, and that it rotates in a cone perpendicular to the membrane. Blatt and Vaz measured the effects of Ca^{2+} on the rotational and translational diffusion of lipids in vesicles on both fast and slow time scales by simultaneously monitoring phosphorescence anisotropy and fluorescence recovery after photobleaching [21]. Below the phase transition temperature (T_m), all motions were slowed with increasing $[Ca^{2+}]$ due to stronger lipid-lipid associations. Above T_m, additional Ca^{2+} resulted in increased flexibility on the phosphorescence time-scale, but reduced mobility on the fluorescence time scale due to structural changes in the lipid/water interface.

Tilley et al. [263] observed the rotational motions of eosin-labeled very-low density, low-density, and high-density lipoproteins. Two motions were observed. The shorter time constant was attributed to segmental flexibility of the chromophore, while the longer time constant reflected overall tumbling. It was observed that the global motion was restricted upon receptor-binding, but the segmental flexibility was maintained even in membrane-bound lipoprotein.

VIID-12. Immunoglobulin E

Zidovetzki et al. [301] studied the rotational mobility of the immunoglobulin E $(IgE)F_c$ receptor complex on rat basophilic leukemia cells. Erythrosin-labeled IgE-receptor complexes exhibited μs relaxation times and a non-zero residual anisotropy indicative of restricted ro-

tational diffusion. The rotational correlation times were found to decrease with increasing temperature from 65 μs at 5.5°C to 23 μs at 38°C. Since the orientational constraint did not change, and no aggregation was observed, this result was attributed to a temperature-dependent change in membrane viscosity.

VIID-13. Nucleic acids

Lavalette et al. covalently labeled 70 S ribosomes with pyrene maleimide or dibromofluorescein isothiocyanate [164]. The rotational time depended upon the concentration of 70 S ribosome, which is suggested to result from an association of the 70 S ribosomes to form 100 S dimers.

Wang et al. [281] monitored the conformational flexibility of DNA in nucleosomes and derived a time constant of 30 ns. Their data were consistent with both twisting motions and nucleosome tumbling. The torsional rigidity for the DNA in the nucleosome was found to be the same as for the uncomplexed DNA, suggesting that nucleosomal DNA retains its twisting flexibility. Hogan et al. [117] used Methylene blue, a DNA-specific intercalator, and Tb^{3+}, a luminescent cation which can replace Ca, to study the structure of nucleosomes. Based upon anisotropy decay and O_2 quenching measurements of Methylene blue it was concluded that there are two distinct classes of Methylene blue in the nucleosome in the presence of Ca. One class appears rigid and accessible to oxygen, and is very similar to Methylene blue intercalated in straight DNA. The second site shows large-scale librational motion and accessibility to oxygen quenching.

Berkoff et al. [17] also probed DNA with oxygen quenching of the triplet probe methylene blue, and concluded that the interior of the dA-dT oligonucleotide is more accessible to small molecules than the dG-dC oligonucleotide. Austin and Jovin [4] labeled RNA polymerase with rose bengal or eosin 5′-isothiocyanate and monitored its anisotropy either in solution or bound in a nonspecific complex with calf thymus DNA or poly[d(A-T)]. In solution, the anisotropy was not single exponential, reflecting a nonspherical shape and complex motions, and was sensitive to salt concentration, consistent with the ionic dependence of dimerization. The anisotropy decay for the protein-DNA complex could be fit with a model in which the DNA exhibits torsional deformation. The authors conclude that their data are inconsistent with a view of DNA as a rigid rod.

VIII. Triplet states used in tissues and cells

VIIIA. Oxygen sensing and phosphorescence imaging

The old saw states that a pessimist sees a glass as half-empty and an optimist sees a glass as half-full. Certainly two divergent views can be held for the effect of molecular oxygen on excited triplet states. When using the triplet state to study macromolecules in solution, the requirement that oxygen be removed represents a technical difficulty. On the other hand, the observed lifetime is a function of the oxygen concentration. Ergo, we can use phosphorescence to detect oxygen, a very important molecule in metabolism! It has already been recognized that the intensity of phosphorescence of a dye in polymers is related to the oxygen concentration [55,124]. If the phosphorescent dye is non-toxic, it can also be used to detect and quantify oxygen in tissues.

As discussed in section VB, quenching is related to the collisional interaction rate of oxygen and the excited-state probe, the lifetime of the excited state and the concentration of oxygen. The longer the lifetime, the more sensitivity to quenching. This relationship has been the rationale to search for molecules with long lifetimes to be used as probes for the quantitative measurement of dioxygen. Pyrene is one of the longest-lived of the fluorescent molecules with a lifetime of approx. 500 ns and it has been used to measure oxygen concentrations in tissues [153,215] and in membranes [81].

Greater sensitivity to oxygen is achieved by using the longer-lived phosphorescence. Ruthenium(II)tris(bipyridyl)ion, with a lifetime of 660 μs, has been used by Sasso et al. to monitor oxygen consumption in enzyme-catalyzed reactions [240]. We have surveyed derivatives of fluorescein and porphyrins for their suitability for measurement of oxygen in solution [268,273]. The phosphorescence lifetimes of these probes were found to depend upon the oxygen concentration by a simple Stern-Volmer relationship with a quenching constant of approx. 10^9 $M^{-1} \cdot s^{-1}$. Binding of the molecules to bovine serum albumin decreased the quenching constant for oxygen by about an order of magnitude and also reduced probe self-quenching, indicating that at the protein binding site the probes are somewhat protected from collision with quenchers. The Pd derivatives of porphyrins were found to have high phosphorescence quantum yield and stability in aqueous solutions and therefore were selected for further studies. Pd coproporphyrin, which is water soluble at the concentrations needed, was used as a phosphorescent indicator to monitor oxygen consumption in reactions catalyzed by glucose oxidase [268,273], in mitochondria [273,287,288] and in cells [286].

In Pd porphyrin the intersystem crossing is very rapid (less than 10 ps, see Holtom and Vanderkooi, unpublished results) and phosphorescence yield is much higher than fluorescence. The high yield of phosphorescence relative to fluorescence allows phosphorescence to be directly measured using a continuous light source. (For most dyes a flash system to gate out

the fluorescence is required before phosphorescence can be seen.) This feature allows a potentially interesting use of phosphorescence – to obtain images of the O_2 distribution in tissue in situ. An example is shown in Fig. 5 where the phosphorescence image of a liver with a low concentration of Pd porphyrin in the perfusate is shown. When the sample is perfused at a high rate with oxygen-containing perfusate, the oxygen levels in the tissue are high, and no phosphorescence can be seen. When the perfusion rate is slowed, the oxygen level in the tissue decreases due to oxygen consumption by the tissue and the phosphorescence intensity increases. The distribution of intensity is not uniform throughout the tissue, areas of high phosphorescence intensity indicating local areas of low oxygen concentrations [236,289]. Phosphorescence measurements of O_2 in tissues offer advantages over conventional techniques in terms of faster time response, precision, sensitivity and ease of imaging the oxygen distribution.

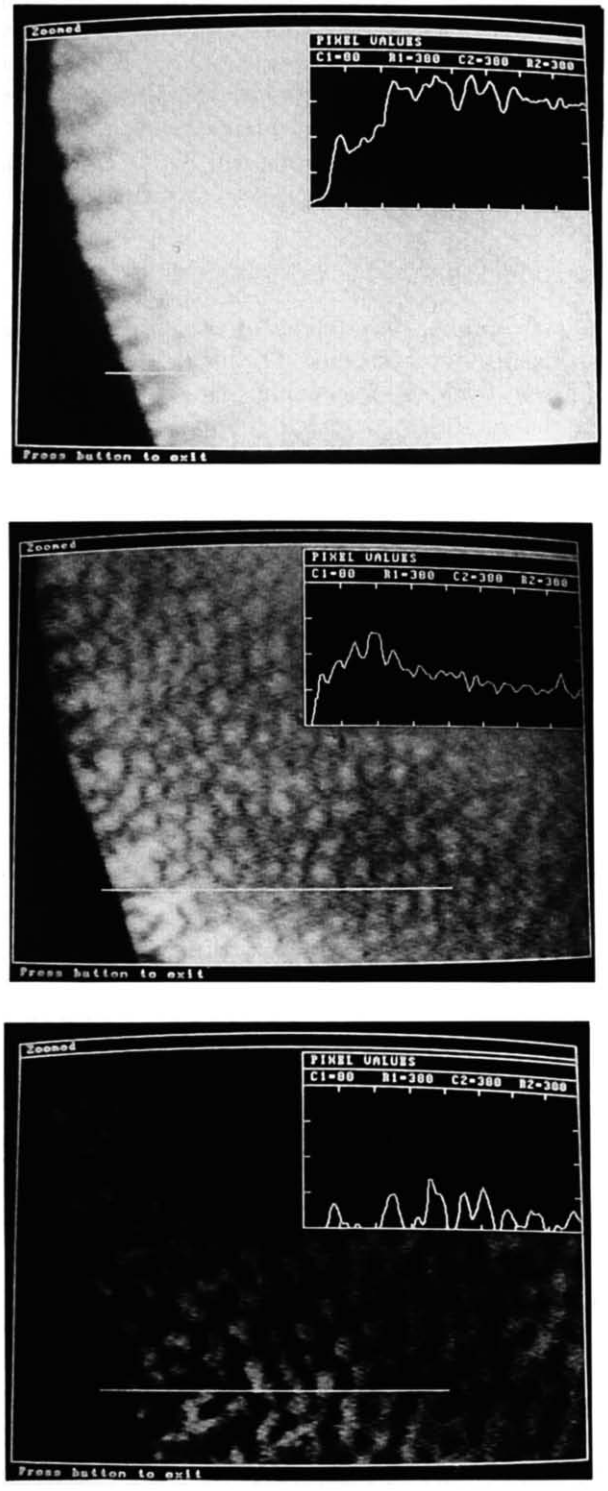

Fig. 5. Phosphorescence images of perfused rat liver. Rat liver was perfused with a medium containing the phosphorescent dye Pd-coproporphyrin. Details are in Ref. 236. Upper: perfusion stopped, and oxygen concentration low; middle: perfusion restarted with oxygenated perfusate; and bottom: after 5 min of perfusion with oxygenated buffer.

VIIIB. Intrinsic phosphorescence from single cells

Mazhul et al. [190] reported that long-lived luminescence could be detected from intact human erythrocytes and white blood cells at ambient temperatures. Tryptophan phosphorescence was observed in bacterial cells by Horie and Vanderkooi [119]. *E. coli* strain k-12, a mutant rich in alkaline phosphatase, exhibited tryptophan phosphorescence with a lifetime comparable to the lifetime of purified alkaline phosphatase, while the wild type which has little alkaline phosphatase showed no detectable phosphorescence on this time scale. The phosphorescence of alkaline phosphatase is very long – about 1.2 s. Thus it was possible to gate faster decaying components of the emission and thereby optically isolate the emission only from alkaline phosphatase.

IX. Summary of the technique; speculations on its further use

The long lifetime of the triplet state allows for measurement of processes which occur on the microsecond-to-second time scale. In concert with fluorescence techniques, picosecond-to-second events can be probed using time-resolved optical spectroscopy with triplet-state techniques, providing access to a time-scale that has been relatively inaccessible. Processes which have been probed with fluorescence techniques, such as rotational motion, translational motion, distances, excited state reactions, and so on, can also be examined with phosphorescence, but on a longer time scale. A consequence of the long lifetime is that reactions that are forbidden (i.e., slow) on the fluorescence time scale can become significant on the phosphorescence time scale. In this regard, the triplet state molecule can be thought of as a separate chemical entity with its own unique chemical properties. The long lifetime of phosphorescence dictates that the lifetime and yield will be very environmentally sensitive. This is seen in the large variation in

phosphorescence lifetimes for proteins at room temperature, which vary by about 5 orders of magnitude. Not only does the lifetime itself reveal important information about the tryptophan site, but the variation in lifetimes implies that emission from a single tryptophan in a multitryptophan assembly can be isolated using temporal gating. For this reason tryptophan phosphorescence should prove to be useful to map distances and mobility even in multitryptophan proteins. A major experimental inconvenience to the measurement of room temperature phosphorescence is the requirement to remove oxygen from the samples. On the other hand, routine deoxygenation schemes have been devised and the oxygen sensitivity of the phosphorescent moiety can itself give information on the chromophore environment. In addition, the sensitivity of phosphorescence to oxygen has been the rationale to use phosphorescence to measure oxygen concentrations. It is clear that phosphorescence measurements have a role in the study of macromolecules and areas for future development are apparent. Because of wide variation in lifetime and spectra, phosphorescence measurements can be made on a single type of chromophore in a mixture of other molecules. In order to capitalize on this specificity, probes that have a specific function, such as interacting with a specific binding site on a macromolecule, could be developed. Examples where fluorescent probes have been synthesized with specific characteristics include the fluorescent chelators of biologically important ions such as Ca^{2+} or Mg^{2+} and derivatives of ATP, NADH and other substrates or cofactors. Similar strategies could be followed for phosphorescent dyes. Phosphorescent derivatives which covalently bind to given residues in proteins or other macromolecules can be used to measure distances. Because phosphorescence involves light, images from it can be obtained by ordinary techniques, such as direct observation or camera. Like fluorescence, phosphorescence measurements can be used on miniature samples, including single cells. For most molecules, the intensity of fluorescence is higher than phosphorescence and gating or phase-shift is needed to eliminate the contribution of the fluorescence in order to obtain fluorescence-free images. Although this is technically feasible it does add complication to the measurement. Alternatively, probes where the phosphorescence/fluorescence intensity is high can be used, and again dyes which are suitable for these measurements can be developed. Finally, structure-function relationships of biomolecules have been examined by determining nuclear positions, and techniques such as X-ray crystallography and nuclear magnetic resonance allow us to determine these. However, reactions occur at the electronic, not the nuclear, level and we need to understand specific electronic relaxation mechanisms. The long-lived decay of the triplet state provides a sensitive tool to examine electronic relaxation processes in biological samples.

Acknowledgements

This work was supported by NIH grants GM 34448 and GM 36393 to J.M.V. and by an NIH Cell and Molecular Biology Training Grant to J.W.B. The authors thank our collegues for helpful comments on the manuscript, including: Drs. S.W. Englander, Judit Fidy, Charles S. Owen, Sandor Papp, William Rumsey and Wayne W. Wright. We thank Ms. Dora Menyhard and Amy Vanderkooi for help in preparing the manuscript. We also thank Drs. W.C. Galley, W.H. Sawyer and G.B. Strambini for sharing with us their unpublished manuscripts.

Note added in proof (June 20, 1989)

A delayed luminescence microscope has recently been described (Jovin, T.M. and Arndt-Jovin, D.J. (1989) Annu. Rev. Biophys. Biophys. Chem. 18, 271–308).

References

1 Adler, M. and Tritton, T.R. (1988) Biophys. J. 53, 989–1005.
2 Alpert, B. and Lindqvist, L. (1975) Science (Washington DC) 187, 836–837.
3 Austin, R.H. and Chan, S.S.L. (1978) Biophys. J. 175–186.
4 Austin, R.H. and Jovin, T. (1983) Biochemistry 22, 3082–3090.
5 Austin, R.H., Chan, S.S. and Jovin, T.M. (1979) Proc. Natl. Acad. Sci. USA 76, 5650–5654.
6 Barboy, N. and Feitelson, J. (1985) Photochem. Photobiol. 41, 9–13.
7 Barboy, N. and Feitelson, J. (1987) Biochemistry 26, 3240–3244.
8 Bartholdi, M., Barrantes, F.J. and Jovin, T.M. (1981) Eur. J. Biochem. 120, 389–397.
9 Beccari, J.B. (1746) Commen. Accad. Bonon. 2, 136–179.
10 Becker, R.S. (1969) Theory and Interpretation of Fluorescence and Phosphorescence, Wiley Interscience, New York, pp. 155–189.
11 Belford, G.G., Belford, R.L. and Weber, G. (1972) Proc. Natl. Acad. Sci. USA 69, 1392–93.
12 Bennett, W.S. and Huber, R. (1984) CRC Crit. Rev. Biochem. 15, 291–384.
13 Bent, D.V. and Hayon, E. (1975) J. Am. Chem. Soc. 97, 2612–2619.
14 Berger, J.W. and Vanderkooi, J.M. (1988) Photochem. Photobiol. 47, 10S.
15 Berger, J.W. and Vanderkooi, J.M. (1989) Biochemistry 28, 5501–5508.
16 Berger, J.W., Vanderkooi, J.M., Tallmadge, D.H. and Borkman, R.F. (1989) Exp. Eye Research, 48, 627–639.
17 Berkoff, B., Hogan, M., Legrange, J. and Austin, R.H. (1986) Biopolymers 25, 307–316.
18 Bishai, F., Kuntz, E. and Augenstein, L. (1967) Biochim. Biophys. Acta 140, 381–394.
19 Bismuto, E., Strambini, G.B. and Irace, G. (1987) Photochem. Photobiol. 45, 741–744.
20 Blatt, E. and Corin, A.F. (1986) Biochim. Biophys. Acta 857, 85–94.
21 Blatt, E. and Vaz, W.L. (1986) Chem. Phys. Lipids 41, 183–94.
22 Blatt, E., Chatelier, R.C. and Sawyer, W.H. (1986) Biophys. J. 50, 349–356.
23 Bolt, J.D. and Turro, N.J. (1982) Photochem. Photobiol. 35, 305–310.
24 Boudin, S. (1930) J. Chim. Phys. 27, 285–290.
25 Bowers, P.G. and Porter, G. (1967) Proc. R. Soc. London., Ser. A 299, 348–353.

26 Buchanan, B.B., Eiermann, W., Riccio, P., Aquila, H. and Klingenberg, M. (1976) Proc. Natl. Acad. Sci. U.S.A. 73, 2280–2284.
27 Burkli, A. and Cherry, R.J. (1981) Biochemistry 20, 138–145.
28 Burghardt, T.P. and Thompson, N.L. (1985) Biochemistry 24, 3731–3735.
29 Burstein, E.A., Vedenkina, N.S. and Ivkova, M.N. (1973) Photochem. Photobiol. 18, 263–279.
30 Callis, J.B., Gouterman, M., Jones, Y.M. and Henderson, B.H. (1971) J. Mol. Spectrosc. 39, 410–420.
31 Calhoun, D.B., Vanderkooi, J.M., Woodrow III, G.V. and Englander, S.W. (1983a) Biochemistry 22, 1526–1532.
32 Calhoun, D.B., Vanderkooi, J.M. and Englander, S.W. (1983b) Biochemistry 22, 1533–1539.
33 Calhoun, D.B., Vanderkooi, J.M., Holtom, G.R. and Englander, S.W. (1986) Proteins 1, 109–115.
34 Calhoun, D.B., Englander, S.W., Wright, W.W. and Vanderkooi, J.M. (1988) Biochemistry 27, 8466–8474.
35 Carapellucci, P.A. and Mauzerall, D. (1975) Ann. New York Acad. Sci. 244, 214–237.
36 Cherry, R.J. (1978) Methods Enzymol. LIV, 47–61.
37 Cherry, R.J. (1979) Biochim. Biophys. Acta 559, 289–327.
38 Cherry, R.J. and Schneider, G. (1976) Biochemistry 15, 3657–61.
39 Cherry, R.J., Burkli, A., Busslinger, M., Schneider, G. and Parish, G.R. (1976a) Nature 262, 389–393.
40 Cherry, R.J., Cogoli, A., Oppliger, M., Schneider, G. and Semenza, G. (1976b) Biochemistry 15, 3653–3656.
41 Cherry, R.J., Heyn, M.P. and Oesterhelt, D. (1977a) FEBS Lett. 78, 25–30.
42 Cherry, R.J., Mueller, U. and Schneider, G. (1977b) FEBS Lett. 80, 465–469.
43 Cherry, R.J., Mueller, U., Holenstein, C. and Heyn, M.P. (1980) Biochim. Biophys. Acta 586, 145–151.
44 Cho, K.C., Che, C.M., Ng, K.M. and Choy, C.L. (1986) J. Am. Chem. Soc. 108, 2814–2818.
45 Churchich, J.E. (1964) Biochim. Biophys. Acta 92, 194–197.
46 Cilento, G. (1984) Pure Appl. Chem. 56, 1179–1190.
47 Cline Love, L.J., Skrilec, M. and Habarta, J.G. (1980) Anal. Chem. 52, 754–759.
48 Cline Love, L.J., Habarta, J.G. and Skrilec, M. (1981) Anal. Chem. 53, 437–444.
49 Closs, G.L., Piotrowiak, P., MacInnis, J.M. and Fleming, G.R. (1988) J. Am. Chem. Soc. 110, 2652–2653.
50 Cone, R.A. (1972) Nature 236, 39–43.
51 Coppey, M., Jameson, D.M. and Alpert, B. (1981) FEBS Lett. 126, 191–194.
52 Corin, A.F. and Jovin, T.M. (1986) Biochemistry 25, 3995–4007.
53 Corin, A.F., Blatt, E. and Jovin, T.M. (1987) Biochemistry 26, 2207–2217.
54 Crutchley, R.J., Ellis Jr., W.R. and Gray, H.B. (1985) J. Am. Chem. Soc. 107, 5002–5004.
55 Czarnecki, S. and Kryszewski, M. (1963) J. Polymer Sci. A1, 3067–3077.
56 Dexter, D.L. (1953) J. Chem. Phys. 21, 836–850.
57 Dixit, S.N., Waring, A.J. and Vanderkooi, J.M. (1981) FEBS Lett. 125, 86–88.
58 Dixit, B.P.S.N., Waring, A., Wells, K., Wong, P., Woodrow, G.V. and Vanderkooi, J.M. (1982) Eur. J. Biochem. 126, 1–9.
59 Dixit, B.P.S.N., Moy, V.T. and Vanderkooi, J.M. (1984) Biochemistry 23, 2103–2107.
60 Domanus, J., Strambini, G.S. and Galley, W.C. (1980) Photochem. and Photobiol., 31, 15–21.
61 Dornmair, K., Corin, A.F., Wright, J.K. and Jahnig, F. (1985) EMBO J. 4, 3633–8.
62 Dufton, M.J., Hider, R.C. and Cherry, R.J. (1984) Eur. Biophys. J., 11, 17–24.
63 Dufton, M.J., Cherry, R.J., Coleman, J.W. and Stanworth, D.R. (1984) Biochem J., 223, 67–72.
64 Eads, T.M., Thomas, D.D. and Austin, R.H. (1984) J. Molec. Biol. 179, 55–81.
65 Eftink, M.R. and Ghiron, C.A. (1975) Proc. Natl. Acad. Sci. 72, 3290–3294.
66 Eftink, M.R. and Ghiron, C.A. (1981) Arch. Biochem. Biophys. 209, 706–709.
67 Eftink, M.R. and Ghiron, C.A. (1981) Photochem. Photobiol. 33, 749–752.
68 Eftink, M.R. and Ghiron, C.A. (1981) Anal. Biochem. 114, 199–227.
69 Eftink, M.R. and Ghiron, C.A. (1984) Biochem. 23, 3891–3899.
70 Eftink, M.R. and Ghiron, C.A. (1987) Photochem. Photobiol. 45, 745–748.
71 Eftink, M.R. and Ghiron, C.A. (1987) Biophys. J. 52, 467–473.
72 Eftink, M.R. and Hagaman, K.A. (1986) Biophys. Chem. 25, 277–282.
73 Eftink, M.R. and Jameson, D.M. (1982) Biochemistry 21, 4443–4449.
74 Ehrenberg, M. and Rigler, R. (1972) Chem. Phys. Lett. 14, 539–44.
75 El-Sayed, M.A., Moomaw, W.R. and Chodak, J.B. (1973) Chem. Phys. Lett. 20, 11–16.
76 Englander, S.W. and Kallenbach, N.R. (1984) Q. Rev. Biophys. 16(4), 521–655.
77 Englander, S.W., Calhoun, D.B. and Englander, J.J. (1987) Analyt. Biochem. 161, 300–306.
78 Favro, L.D. (1960) Phys. Rev. 119, 53–60.
79 Feitelson, J. and Mauzerall, D. (1982) J. Phys. Chem. 86, 1623–1628.
80 Finazzi-Agro, A., Zolla, L., Flamigni, L., Kuiper, H.A. and Brunori, M. (1982) Biochemistry 21, 415–418.
81 Fischkoff, S. and Vanderkooi, J.M. (1975) J. Gen. Physiol. 65, 663–676.
82 Frauenfelder, H., Petsko, G.A. and Tsernoglou, D. (1979) Nature 280, 558–563.
83 Friend, S.H. and Gurd, F.R.N. (1979) Biochemistry 18, 4612–4619.
84 Förster, T. (1948) Ann. Phys. (Leipzig) 2, 55–75.
85 Fujiwara, T. and Nagayama, K. (1985) J. Chem. Phys. 83, 3110–17.
86 Gabellieri, E., Strambini, G.B. and Gualtieri, P. (1988) Biophys. Chem. 30, 61–67.
87 Garland, P.B. and Birmingham, J.J. (1986) in Applications of Fluorescence in the Biomedical Sciences (D.L. Taylor, A.S. Waggoner, F. Lanni, R.F. Murphy, R.R. Birge, eds.), Alan R. Liss, New York, pp. 245–254.
88 Garland, P.B. and Moore, C.H. (1979) Biochem. J. 183, 561–572.
89 Geacintov, N.E., Flamer, T.J., Prusik, T. and Khosrofian, J.M. (1975a) Biochem. Biophys. Res. Commun. 64, 1245–1252.
90 Geacintov, N.E., Prusik, T. and Khosrofian, J.M. (1975b) J. Am. Chem. Soc. 98, 6444–6452.
91 Geacintov, N.E., Waldmeyer, J., Kuzmin, V.A. and Kolubayev, T. (1981) J. Phys. Chem. 85, 3608–3613.
92 Georghiou, S., Thompson, M. and Mukhopadhyay, A.H. (1981) Biochim. Biophys. Acta 642, 429–432.
93 Ghiron, C., Bazin, M. and Santus, R. (1988) Biochim. Biophys. Acta 957, 207–216.
94 Ghiron, C., Bazin, M. and Santus, R. (1988) Photochem. Photobiol. 48, 539–543.
95 Gijzeman, O.L.J., Kaufman, F. and Porter, G. (1973) J. Chem. Soc. Faraday Trans. II, 69, 708–720.
96 Gioannini, T.L. and Campbell, P. (1980) Biochem. Biophys. Res. Comm. 96, 106–113.
97 Gonnelli, M. and Strambini, G.B. (1986) Biophys. Chem. 24, 161–167.
98 Gouterman, M. in The Porphyrins III (1979) (D. Dolphin, ed.), pp. 1–165, Academic Press, New York.

99 Gradyushko, A.T. and Tsvirko, M.P. (1961) Opt. Spectrosc. (Engl. Transl.) I, 91–111.
00 Gratton, E., Alpert, B., Jameson, D.M. and Weber, G. (1984) Biophys. J. 45, 789–794.
01 Green, T.J., Wilson, D.F., Vanderkooi, J.M. and DeFeo, S.P., (1988) Analyt. Biochem. 174, 73–79.
02 Greinert, R., Staerk, H., Stier, A. and Weller, A. (1979) J. Biochem. Biophys. Meth. 1, 77–83.
03 Grinvald, A. and Steinberg, I.Z. (1976) Biochim. Biophys. Acta 427, 663–678.
04 Grossweiner, L.I. (1956) J. Chem. Phys. 24, 1255–1256.
05 Gupte, S., Wu, E.-S., Hochli, L., Moechli, M., Jacobson, K., Sowers, A.E. and Hackenbrock, C.R. (1984) Proc. Natl. Acad. Sci. USA 81, 2606–2610.
06 Gut, J., Richter, C., Cherry, R.J., Winterhalter, K.H. and Kawato, S. (1982) J. Biol. Chem. 257, 7030–7036.
07 Gut, J., Richter, C., Cherry, R.J., Winterhalter, K.H. and Kawato, S. (1983) J. Biol. Chem. 258, 8588–8594.
08 Harris, D.T. (1926) Biochem. J. 20, 288–292.
09 Hastings, J.W. and Gibson, Q.H. (1967) J. Biol. Chem. 242, 720–726.
10 Hicks, B., White, M., Ghiron, C.A., Kuntz, R.R. and Volker, W.A. (1978) Proc. Natl. Acad. Sci. USA 75, 1172–1175.
11 Ho, P.S., Sutoris, C., Liang, N., Margoliash, E. and Hoffman, B.M. (1985) J. Am. Chem. Soc. 107, 1070–1071.
12 Hochman, J.H., Schindler, M., Lee, J.G. and Ferguson-Miller, S. (1982) Proc. Natl. Acad. Sci. USA 79, 6866–6870.
13 Hoffmann, W., Sarzala, M.G. and Chapman, D. (1979) Proc. Natl. Acad. Sci. 76, 3860–3864.
14 Hogan, M., Wang, J., Austin, R.H., Monitto, C. and Hershkowitz, S. (1982) Proc. Natl. Acad. Sci. USA 79, 3518–3522.
15 Hogan, M., Austin, R.H. and Legrange, J. (1983) CIBA Found. Symp. 93, 226–45.
16 Hogan, M.E., Hayes, B., Wang, N.C. and Austin, R.H. (1986) Biochemistry 25, 5070–82.
17 Hogan, M.E., Rooney, T.F. and Austin, R.H. (1987) Nature 328(B130), 554–557.
18 Hopf, F.R. and Whitten, D.G. (1978) in The Porphyrins II (D. Dolphin, ed.), Ch. 6, pp. 161–195, Academic Press, New York.
19 Horie, T. and Vanderkooi, J.M. (1981) Biochim. Biophys. Acta 670, 290–297.
20 Horie, T. and Vanderkooi, J.M. (1982) FEBS Lett. 147, 69–73.
21 Horie, T. and Vanderkooi, J.M. (1984) Life Sciences Rep. 2, 141–178.
22 Horie, T., Maniara, G. and Vanderkooi, J.M. (1984) FEBS lett. 177, 287–290.
23 Horie, T., Vanderkooi, J.M. and Paul, K.G. (1985) Biochemistry 24, 7935–7941.
24 Hormats, E.I. and Unterleitner, F.C. (1965) J. Phys. Chem. 69, 3677–3681.
25 Ishiwata, S., Kinosita, K., Yoshimura, H. and Ikegami, A. (1987) Biol. Chem. 262, 8314–8317.
26 Jablonski, A. (1935) Z. Phys. 94, 38–46.
27 Jackson, G. and Porter, G. (1961) Proc. R. Soc. (London) A 260, 13–30.
28 Jameson, D.M., Gratton, E., Weber, G. and Alpert, B. (1984) Biophys. J. 45, 795–803.
29 Johnson, P. and Garland, P.B. (1981) FEBS Lett. 132, 252–56.
30 Johnson, P.J. and Garland, P.B. (1982) Biochem. J. 203, 313–21.
31 Joshi, N., Johnson, M.L., Gryczynski, I. and Lakowicz, J.R. (1987) Chem. Phys. Lett. 135, 200–207.
32 Jovin, T.M. (1988) Biochem. Soc. Trans., 14(5), 817–818.
33 Jovin, T.M., Bartholdi, M., Vaz, W.L.G. and Austin, R.M. (1981) Ann. NY Acad. Sci. 366, 176–196.
34 Junankar, P.P. and Cherry, R.J. (1986) Biochim. Biophys. Acta 854, 198–206.
35 Junge, W. (1972) FEBS Lett. 25, 109–112.
136 Junge, W. and Devault, D. (1975) Biochim. Biophys. Acta 408, 200–14.
137 Kai, Y. and Imakubo, K. (1979) Photochem. Photobiol. 29, 261–265.
138 Kalyanasundaram, K., Grieser, F. and Thomas, J.K. (1977) Chem. Phys. Lett. 51, 501–505.
139 Kanagy, C., Vanderkooi, J.M. and Bonner Jr., W.D. (1988) Arch. Biochem. Biophys., 267, 668–675.
140 Karplus, M. (1986) Methods Enzymol. 131, 283–307.
141 Kautsky, H. (1939) Trans. Faraday Soc. 35, 216–219.
142 Kautsky, H. and Muller, G.O. (1947) Z. Naturforsch 2a, 167–172.
143 Kawato, S., Sigel, E., Carafoli, E. and Cherry, R.J. (1980) J. Biol. Chem. 255, 5508–5510.
144 Kawato, S., Sigel, E., Carafoli, E. and Cherry, R.J. (1981) J. Biol. Chem. 256, 7518–7527.
145 Kawato, S., Lehner, C., Muller, M. and Cherry, R.J. (1982a) J. Biol. Chem. 257, 6470–6476.
146 Kawato, S., Gut, J., Cherry, R.J., Winterhalter, K.H. and Ritcher, C. (1982b) J. Biol. Chem. 257, 7023–7029.
147 Kim, H. and Galley, W.C. (1983) Can. J. Biochem. 61, 46–53.
148 Kinosita, K., Kawato, S. and Ikegami, A. (1977) Biophys. J. 20, 289–305.
149 Kinosita, K., Ikegami, A. and Kawato, S. (1982) Biochem. J. 37, 461–464.
150 Kinosita, K., Ishiwata, S., Yoshimura, H., Asai, H. and Ikegami, A. (1984) Biochem. 23, 5963–5975.
151 Kishner, S., Trepman, W. and Galley, W.C. (1983) Can. J. Biochem. 57, 1299–1304.
152 Klingenberg, M., Riccio, P., Aquila, H., Buchanan, B.B. and Grebe, K. (1975) in Mechanism of Carrier Transport and the ADP, ATP Carrier (Hatefi, Y. and Djavadi-Ohaniance, L., eds.), pp. 341–348, Elsevier/North-Holland, Amsterdam.
153 Knopp, J.A. and Longmuir, I.W. (1972) Biochim. Biophys. Acta 279, 393–397.
154 Koloczek, H. and Vanderkooi, J.M. (1987) Biochem. Biophys. Acta 916, 236–244.
155 Koloczek, H., Horie, T., Yonetani, T., Anni, H., Maniara, G. and Vanderkooi, J.M. (1987) Biochemistry 26, 3142–3148.
156 Konev, S.V. (1967) Fluorescence and Phosphorescence of Proteins and Nucleic Acids, Plenum Press, New York.
157 Krupjanskii, Y., Parak, F., Goldanskii, V.I., Mossbauer, R.L., Gaubmann, E.E., Engelmann, H. and Suzdalev, I.P. (1982) Z. Nat. Forsch. 37c, 57–62.
158 Kunze, U. and Junge, W. (1977) FEBS Lett. 80, 429–434.
159 Lakowicz, J.R. (1983) Principles of Fluorescence, pp. 52–89, Plenum Press, New York.
160 Lakowicz, J.R. and Weber, G. (1973) Biochemistry 12, 4171–4179.
161 Lakowicz, J.R. and Weber, G. (1980) Biophys. J. 32, 591–600.
162 Lakowicz, J.R., Maliwal, B.P., Cherek, H. and Balter, A. (1983) Biochemistry 22, 1741–1752.
163 Larralde, C., Sassa, S., Vanderkooi, J.M., Koloczek, H., Laclette, J.P., Goodsaid, F., Sciutto, E. and Owen, C.S. (1987) Molec. Biochem. Parasitol. 22, 203–213.
164 Lavalette, D., Amand, B. and Pochon, F. (1977) Proc. Natl. Acad. Sci. USA 74, 1407–1411.
165 Leaver, I.H. (1978) Photochem. Photobiol. 27, 439–443.
166 Lee, P.M., Cherry, R.J. and Baechi, T. (1983) Virology 128, 65–76.
167 Lee, W.E. and Galley, W.C. (1988) Biophys. J. 54, 627–635.
168 Lewis, G. and Calvin, M. (1945) J. Am. Chem. Soc. 67, 1232–1233.
169 Lewis, G. and Kasha, M. (1944) J. Am. Chem. Soc. 66, 2100–2116.
170 Lewis, G., Lipkin, D. and Magel, T. (1961) J. Am. Chem. Soc. 63, 3005–3018.
171 Liang, N., Kang, C.H., Ho, P.S., Margoliash, E. and Hoffman, B.M. (1986) J. Am. Chem. Soc. 108, 4665–4666.
172 Liang, N., Pielak, G.J., Mauk, A.G., Smith, M. and Hoffman, B.M. (1987) Proc. Natl. Acad. Sci. USA 84,1249–1252.

173 Liang, N., Mauk, A.G., Pielak, G.J., Johnson, J.A., Smith, M. and Hoffman, B.M. (1988) Science 240, 311–313.
174 Lindsey, J.S. and Mauzerall, D.C. (1983) J. Am. Chem. Soc. 105, 6528–6529.
175 Lindroth, J.R., Martin, S.M. and Ledbetter, J.W. (1987) Comput. Biol. Med. 17, 369–381.
176 Lipari, G. and Szabo, A. (1980) Biophys. J. 30, 489–506.
177 Lipari, G. and Szabo, A. (1981) J. Chem. Phys. 2971–2976.
178 Lo, M., Garland, P.B., Lamprecht, J. and Barnard, E.A. (1980) FEBS Lett. 111, 407–412.
179 Longworth, J.W. (1971) in Excited States of Proteins and Nucleic Acids (Steiner, R.F. and Weinryb, G., eds.), pp. 319–484, Plenum Press, New York.
180 Lower, S.K. and El-Sayed, M.A. (1966) Chem. Rev. 66, 199–241.
181 Ludescher, R.D. and Thomas, D.D. (1988) Biochemistry 27, 3343–3351.
182 Ludescher, R.D., Eads, T.M. and Thomas, D.D. (1986) Optical Studies of Muscle Cross Bridges, (Baskin, R.J. and Yeh, Y., eds.), pp. 33–65, CRC Press, Boca Raton, FL.
183 Ludescher, R.D., Eads, T.M. and Thomas, D.D. (1988) J. Mol. Biol. 200, 89–99.
184 Maniara, G., Bloomgarden, D., Vanderkooi, J.M. and Koloczek, H. (1987) Photochem. Photobiol. 47, 207–208.
185 Marcus, R.A. (1956) J. Chem. Phys. 24, 966–978.
186 Marcus, R. (1982) Faraday Soc. Discuss. 74, 1–10.
187 Marcus, R.A. and Sutin, N. (1985) Biochim. Biophys. Acta 811, 265–322.
188 Mauzerall, D. (1978) in The Porphyrins V. (D. Dolphin, ed.), pp. 29–52, Academic Press, New York.
189 Mayo, S.L., Ellis Jr., W.R., Crutchley, R.J. and Gray, H.B. (1986) Science 233, 948–52.
190 Mazhul, V.M., Elmolaev, Y.S. and Konev, S.V. (1980) Zh. Prikl. Spektrosk. 32, 903–906.
191 McCammon, J.A. and Northrup, S.H. (1981) Nature (Lond.) 293, 316–317.
192 McClure, D. (1949) J. Chem. Phys. 17, 905–913.
193 McClure, D.S., Blake, N.W. and Hanst, P.L. (1954) J. Chem. Phys. 22, 255–258.
194 McGlynn, S.P., Azumi, T. and Kinoshita, M. (1969) Molecular Spectroscopy of the Triplet State, Prentice-Hall, Englewood Cliffs, NJ.
195 McIntosh, P.R., Kawato, S., Freedman, R.B. and Cherry, R.J. (1980) FEBS Lett. 122, 54–58.
196 McLendon, G.L. and Miller, J.R. (1985) J. Am. Chem. Soc. 107, 7811–7816.
197 McLendon, G.L., Winkler, J.R., Nocera, D.G., Mauk, M.R., Mauk, A.G. and Gray, H.B. (1985) J. Am. Chem. Soc. 107, 739–740.
198 Milton, J.G. and Galley, W.C. (1986) Biopolymers 25, 1673–1683.
199 Moore, C.H. and Garland, P.B. (1979) Biochem. Soc. Trans. 7, 945–946.
200 Moore, C., Boxer, D. and Garland, P. (1979) FEBS Lett. 108, 161–166.
201 Muehlebach, T. and Cherry, R.J. (1982) Biochemistry 21, 4225–4228.
202 Muhlebach, T. and Cherry, R.J. (1985) Biochemistry 24, 975–983.
203 Müller, M., Krebs, J.J.R., Cherry, R.J. and Kawato, S. (1982) J. Biol. Chem. 257, 1117–1120.
204 Müller, M., Krebs, J.J.R., Cherry, R.J. and Kawato, S. (1984) J. Biol. Chem. 259, 3037–3043.
205 Munro, I., Pecht, I. and Stryer, L. (1979) Proc. Natl. Acad. Sci. USA 76, 56–60.
206 Murray, E.K., Restall, C.J. and Chapman, D. (1983) Biochim. Biophys. Acta 732, 347–351.
207 Mauzerall, D. (1973) Ann. NY Acad. Sci. 206, 64–72.
208 Nigg, E.A. and Cherry, R.J. (1979) Biochemistry 18, 3457–3465.
209 Nigg, E. and Cherry, R.J. (1979b) Nature 277, 493–49.
210 Nigg, E.A. and Cherry, R.J. (1980) Proc. Natl. Acad. Sci. U 77, 4702–4706.
211 Nigg, E., Kessler, M. and Cherry, R.J. (1979a) Biochim. Bioph Acta 550, 328–340.
212 Nigg, E.A., Gahmberg, C.G. and Cherry, R.J. (1980) Bioch Biophys. Acta. 600, 636–642.
213 Nocera, D.G., Winkler, J.R., Yocum, K.M., Bordignon, E. a Gray, H.B. (1984) J. Am. Chem. Soc. 106, 6145–5150.
214 Noyes, R.M. (1961) in progress in Reaction Kinetics, Vol. I., 131–148, Pergamon Press, Oxford.
215 Opitz, N. and Lubbers, D.W. (1984) Adv. Exp. Med. Biol. 1 261–267.
216 Reference deleted.
217 Parker, C.A. (1968) Photoluminescence of Solutions, Elsev Amsterdam.
218 Parker, C.A. and Hatchard, C.G. (1961) Trans. Faraday Soc., 1894–1904.
219 Parker, C.A. and Hatchard, C.G. (1963) Trans. Faraday Soc. 284–295.
220 Parker, C.A. and Joyce, T.A. (1967) Photochem. Photobiol. 396–406.
221 Parker, C.A. and Joyce, T.A. (1973) Photochem. Photobiol. 467–474.
222 Perrin, F. (1936) J. Phys. Radium (Paris) 7, 1–11.
223 Pepmiller, C., Bedwell, E., Kuntz, R.R. and Ghiron, C.A. (19 Photochem. Photobiol. 38, 273–280.
224 Peterson-Kennedy, S.E., McGourty, J.L., Kalweit, J.A. and Hc man, B.M. (1986) J. Am. Chem. Soc. 108, 1739–1746.
225 Petrich, J.W., Longworth, J.W. and Fleming, G.R. (1987) B chemistry 26, 2711–2722.
226 Prusik, T., Geacintov, N.E., Tobiasz, C., Ivanovic, V. and We stein, I.B. (1979) Photochem. Photobiol. 29, 223–232.
227 Purugganan, M.D., Kumar, C.V., Turro, N.J. and Barton, J. (1988) Science 241, 1645–1649.
228 Razi Naqvi, K., González-Rodríguez, J., Cherry, R.J. and Cha man, D. (1973) Nature New Biology 245, 249–251.
229 Restall, C.J., Dale, R.E., Murray, E.K., Glibert, C.W. and Cha man, D. (1984) Biochemistry 23, 6765–6776.
230 Restall, C.J., Coke, M., Murray, E.K. and Chapman, D. (19 Biochim. Biophys. Acta, 813, 96–102.
231 Richards, F.M. (1979) Carlsberg Res. Commun. 44, 47–63.
232 Richter, C., Winterhalter, K.H. and Cherry, R.J. (1979) FE Lett. 102, 151–154.
233 Rigler, R. and Ehrenberg, M. (1973) Q. Rev. Biophys. 6, 139–1
234 Robbins, R.J., Fleming, G.R., Beddard, G.S., Robinson, G.\ Thistlewaite, P.J. and Woolfe, G.J. (1980) J. Am. Chem. Soc. 1 6271–6279.
235 Ross, J.B.A., Schmidt, C.J. and Brand, L. (1981) Biochemistry 4369–4377.
236 Rumsey, W.L., Vanderkooi, J.M. and Wilson, D.F. (1988) S ence, 241, 1649–1651.
237 Rupley, J.A., Gratton, E. and Careri, G. (1983) Trends Bioche Sci. 8, 18–22.
238 Saffman, P.G. and Delbruk, M. (1975) Proc. Natl. Acad. S USA 72, 3111–3113.
239 Saltiel, J. and Atwater, B.W. (1988) Adv. Photochem. 14, 1–
240 Sasso, M.G., Quina, F.H. and Bechara, E.J.H. (1986) An Biochem. 156, 239–243.
241 Sawyer, W.H., Woodhouse, A.G., Czarnecki, J.J. and Blatt, (1988) Biochemistry 28, 7733–7740.
242 Saviotti, M.L. and Galley, W.C. (1974) Proc. Natl. Acad. S USA, 71, 4154–4158.
243 Schenk, C.C., Blankenship, R.E. and Parson, W.W. (1982) B chim. Biophys. Acta 680, 44–59.
244 Sidki, A.M., Smith, D.S. and Landon, J. (1986) Clin. Chem. 53–56.
245 Siebrand, W. (1967) J. Chem. Phys. 47, 2411–2422.

246 Smoluchowski, M. (1918) Z. Physik. Chem. (Leipzig). 92, 129–168.
247 Somogyi, B., Norman, J.A. and Rosenberg, A. (1986) Biophys. J. 50, 55–61.
248 Speirs, A., Moore, C.H., Boxer, D.H. and Garland, P.B. (1983) Biochem. J. 213, 67–74.
249 Stern, O. and Volmer, M. (1919) Phys. Z. 20, 183–188.
250 Steiner, R.F. (1983) in Excited States of Biopolymers (Steiner, R.F., ed.) Plenum Press, NY. pp. 117–160.
251 Strambini, G.B. (1983) Biophys. J. 43, 127–130.
252 Strambini, G.B. (1987) Biophys. J. 52, 23–28.
253 Strambini, G.B. and Gabellieri, E. (1984) Photochem. Photobiol. 39, 725–729.
254 Strambini, G.B. and Gabellieri, E. (1987) Biochemistry 26, 6527–6530.
255 Strambini, G.B. and Galley, W.C. (1976) Nature (Lond.) 260, 554–556.
256 Strambini, G.B. and Galley, W.C. (1980) Biopolymers 19, 383–394.
257 Strambini, G.B. and Gonnelli, M. (1985) Chem. Phys. Lett. 115, 196–200.
258 Strambini, G.B. and Gonnelli, M. (1986) Biochemistry 25, 2471–6.
259 Strambini, G.B., Cioni, P. and Felicioli, R.A. (1987) Biochemistry 26, 4968–2975.
260 Stryer, L. and Haugland, R.P. (1967) Proc. Natl. Acad. Sci. 58, 719–726.
261 Szabo, A. (1984) J. Chem. Phys. 81, 150–167.
262 Tao, T. (1969) Biopolys. 8, 609–632.
263 Tilley, L., Sawyer, W.H., Morrison, J.R. and Fidge, N.H. (1988) J. Biol. Chem. 263, 17541–16547.
264 Thomas, D.D., Carlsen, W.F. and Stryer, L. (1978) Proc. Natl. Acad. Sci. USA 75, 5746–5750.
265 Turro, N.J. (1978) Modern Molecular Photochemistry (The Benjamin/Cummings Publishing Co., Inc.) pp. 296–361, Menlo Park, CA.
266 Turro, M.J., Cox, G.S. and Li, X. (1963) Photochem. Photobiol. 37, 149–153.
267 Vadas, E.B., Melancon, P., Braun,P.E. and Galley, W.C. (1981) Biochemistry 20, 3110–3116.
268 Vanderkooi, J.M. and Wilson, D.F. (1986) Adv. Expl. Med. Biol. 200, 189–193.
269 Vanderkooi, J.M., Fischkoff, S., Andrich, M., Podo, F. and Owen, C.S. (1975) J. Chem. Phys. 63, 3661–3666.
270 Vanderkooi, J.M., Adar, F. and Erecinska, M. (1976) Eur. J. Biochem. 64, 381–387.
271 Vanderkooi, J.M., Maniara, G. and Erecinska, M. (1985) J. Cell Biol. 100, 435–441.
272 Vanderkooi, J.M., Calhoun, D.B. and Englander, S.W. (1987a) Science 236, 568–569.
273 Vanderkooi, J.M., Maniara, G., Green, T.J. and Wilson, D.F. (1987b) J. Biol. Chem. 262, 5476–5482.
274 Vanderkooi, J.M., Papp, S., Samoriski, T., Pikula, S. and Martonosi, A. (1989) Biochem. Biophys. Acta 957, 230–236.
275 Van Gunsteren, W,F. and Karplus, M. (1982) Biochemistry 21, 2255–2273.
276 Van Hoogevest, P., De Kruijff, B. and Garland, P.B. (1985) Biochim. Biophys. Acta 813, 1–9.
277 Vaz, W.L.C., Austin, R.H. and Vogel, H. (1979) Biophys. J. 26, 415–426.
278 Vo-Dinh, T. and Uziel, M. (1987) Anal. Chem. 59, 1093–5.
279 Vos, K., Lavalette, D. and Visser, A.J.W.G. (1987) Eur. J. Biochem. 169, 269–273.
280 Wahl, P. (1983) in Time-resolved Fluorescence Spectroscopy in Biochemistry and Biology (Cundall, R. and Dale, R., eds.), pp. 483–496, Plenum Press, New York.
281 Wang, N.C., Hogan, M.E. and Austin, R.H. (1982) Proc. Natl. Acad. Sci. USA 79, 5896–5900.
282 Ware, W.R. and Novros, J.S. (1966) J. Phys. Chem. 70, 3246–3253.
283 Weber, G. (1952) Biochem. J. 51, 145–155.
284 Weber, G. (1953) Adv. Protein Chem. 8, 415–459.
285 Wegener, W.A. (1984) Biophys. J. 46, 795–803.
286 Wilson, D.F. and Rumsey, W.L. (1988) Adv. Exptl. Med. Biol. 222, 121–131.
287 Wilson, D.F., Vanderkooi, J.M., Green, T.J., Maniara, G., Defeo, S.P. and Bloomgarden, D.C. (1987) Adv. Exp. Med. Biol. 215, 71–77.
288 Wilson, D.F., Rumsey, W.L., Green, T.J. and Vanderkooi, J.M. (1988) J. Biol. Chem. 263, 2712–2718.
289 Wilson, D.F., Rumsey, W.L. and Vanderkooi, J.M. (1989) Adv. Exptl. Med. Biol., in press.
290 Reference deleted.
291 Yguerabide, J., Epstein, H.F. and Stryer, L. (1970) J. Mol. Biol. 51, 573–90.
292 Yocom, K.T., Shelton, J.B., Shelton, J.R., Schroeder, W.A., Worosila, G., Isied, S.S., Bordignon, E. and Gray, H.B. (1982) Proc. Natl. Acad. Sci. USA 79, 7052–7055.
293 Yonetani, T. and Asakura, T. (1968) J. Biol. Chem. 243, 3996–3998.
294 Yoshida, T.M. and Barisas, B.G. (1986) Biophys. J. 50, 41–53.
295 Yoshida, T.M., Zarrin, F. and Barisas, B.G. (1988) Biophys. J. 54, 277–288.
296 Yoshimura, H., Nishio, T., Mihashi, K., Kinosita, K. and Ikegami, A. (1984) J. Mol. Biol. 179, 453–467.
297 Youtsey, K.J. and Grossweiner, L.I. (1967) Photochem. Photobiol. 6, 721–731.
298 Yudanova, Y., Meckler, V., Goel, V., Kulikov, A., Kotelmikov, A., Liktenstein, G., Berkovich, M., Karyakin, A., Archakov, A., Kaplun, A. and Schvets, V. (1986) Eur. J. Biochem. 156, 541–544.
299 Zemel, H. and Hoffman, B.M. (1981) J. Am. Chem. Soc. 103, 1192–1201.
300 Zidovetzki, R., Yarden, Y., Schlessinger, J. and Jovin, T.M. (1981) Proc. Nat. Acad. Sci. 78, 6981–6985.
301 Zidovetzki, R., Bartholdi, M., Arndt-Jovin, D. and Jovin, T.M. (1986a) Biochemistry 25, 4397–4401.
302 Zidovetzki, R., Yarden, Y., Schlessinger, J. and Jovin, T.M. (1986b) EMBO J. 5, 247–250.